DISTILLATION

1. Introduction

Distillation is a method of separation that is based on the difference in composition between a liquid mixture and the vapor formed from it. This composition difference arises from the dissimilar effective vapor pressures, or volatilities, of the components of the liquid mixture. When such dissimilarity does not exist, as at an azeotropic point, separation by simple distillation is not possible. Distillation as normally practiced involves condensation of the vaporized material, usually in multiple vaporization/condensation operations, and thus differs from evaporation (qv), which is usually applied to separation of a liquid from a solid but which can be applied to simple liquid concentration operations.

Distillation is the most widely used industrial method of separating liquid mixtures and is at the heart of the separation processes in many chemical and petroleum plants (see SEPARATION PROCESS SYNTHESIS). The most elementary form of the method is simple distillation, in which the liquid is brought to boiling and the vapor formed is separated and condensed to form a product. If the process is continuous with respect to feed and product flows, it is called flash distillation. If the feed mixture is available as an isolated batch of material, the process is a form of batch distillation and the compositions of the collected vapor and residual liquid are thus time dependent. The term fractional distillation, which may be contracted to fractionation, was originally applied to the collection of separate fractions of condensed vapor, each fraction being segregated. In modern practice the term is applied to distillation processes in general, where an effort is made to separate an original mixture into several components by means of distillation. When the vapors are enriched by contact with counterflowing liquid reflux, the process is often called rectification. When fractional distillation is accomplished with a continuous feed of material and continuous removal of product fractions, the process is called continuous distillation. When steam (qv) is added to the vapors to reduce the partial pressures of the components to be separated, the term steam distillation is used.

Most distillations conducted commercially operate continuously, with a more volatile fraction recovered as distillate and a less volatile fraction recovered as bottoms or residue. If a portion of the distillate is condensed and returned to

the process to enrich the vapors, the liquid is called reflux. The apparatus in which the enrichment occurs is usually a vertical, cylindrical vessel called a still or distillation column. This apparatus normally contains internal devices for effecting vapor–liquid contact; the devices may be categorized as plates or packings.

Distillation has been practiced in one form or another for centuries. It was of fundamental importance to the alchemists and was in use well before the time of Christ. The historical development of distillation has been published (1) as has the history of vapor–liquid contacting devices (2).

2. Vapor–Liquid Equilibria

The equilibrium distributions of mixture component compositions in the vapor and liquid phases must be different if separation is to be made by distillation. It is important, therefore, that these distributions be known. The compositions at thermodynamic equilibrium are termed vapor–liquid equilibria (VLE) and may be correlated or predicted with the aid of thermodynamic relationships. The driving force for any distillation is a favorable vapor–liquid equilibrium, which provides the needed composition differences. Reliable VLE are essential for distillation column design and for most other operations involving liquid–vapor phase contacting. Many VLE have been measured and reported in the literature, and compilations of such data are available (3,4). Also, bibliographic guides have been published, providing source references for thousands of publications presenting VLE (5–7). If data are not to be found, they may be measured, or estimated by generalized methods (8–10), with some sacrifice in reliability. Even if carefully measured data are available, thermodynamic models are usually required to extrapolate or interpolate the data for conditions not

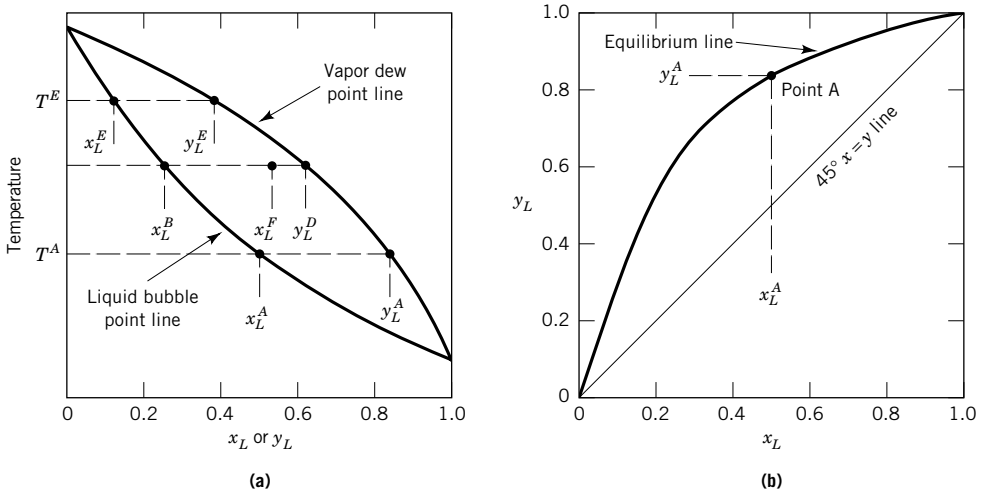

Fig. 1. Isobaric VLE diagrams: (**a**) dew and bubble point; (**b**) vapor–liquid (y–x) equilibrium.

represented by the experiments. Whatever the source and extent of the VLE, some evaluation should be made with regard to accuracy.

The VLE for the system at hand may be simple and easily represented by an equation or, in some systems, may be so complex that they cannot be adequately measured or represented. Excellent treatises are available for selection and implementation of vapor–liquid equilibrium studies (11–14). Typical VLE for binary systems are shown graphically in Figure 1. Figure 1**a** is a representative boiling-point diagram showing equilibrium compositions as functions of temperature at a constant pressure. The lower line is the liquid bubble point line, the locus of points at which a liquid on heating forms the first bubble of vapor. The upper line is the vapor dew-point line, representing points at which a vapor on cooling forms the first drop of condensed liquid. The liquid and vapor compositions are conventionally plotted in terms of the low-boiling (more volatile) substance, L, in the mixture. The system point A has a vapor composition of $y_L{}^{A}$ in equilibrium with a liquid composition of $x_L{}^{A}$ at a temperature of T^{A}. Figure 1**b** is a typical isobaric phase or y–x diagram. For further discussion, several textbooks are available (15,16).

2.1. Thermodynamic Relationships. A closed container with vapor and liquid phases at thermodynamic equilibrium may be depicted as in Figure 2, where at least two mixture components are present in each phase. The components distribute themselves between the phases according to their relative volatilities. A distribution ratio for mixture component i may be defined using mole fractions:

$$K_i = y_i{}^{*}/x_i \tag{1}$$

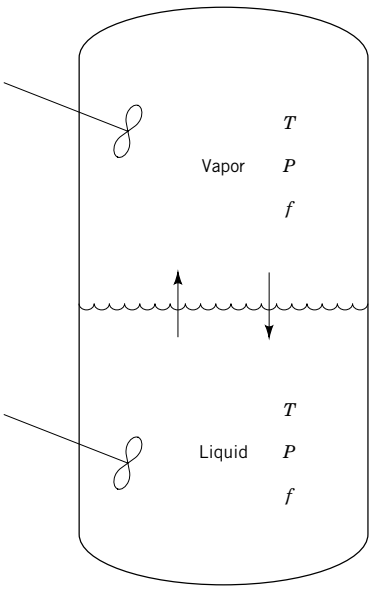

Fig. 2. Equilibrium between vapor and liquid. The conditions for equilibrium are $T^{V} = T^{L}$ and $P^{V} = P^{L}$. For a given T and P, phase fugacities are equal, ie, $f^{V} = f^{L}$ and $f_i{}^{V} = f_i{}^{L}$.

where the asterisk is used to denote an equilibrium condition. This K term, known as the vapor–liquid equilibrium ratio, or often the K value, is widely used, especially in the petroleum (qv) and petrochemical industries. For any two mixture components i and j, their relative volatility, often called the alpha value, is defined as

$$\alpha_{ij} = \frac{K_i}{K_j} = \frac{y_i x_j}{x_i y_j} = \frac{y_i(1-x_i)}{x_i(1-y_i)} \tag{2}$$

Equation 2 may be rearranged to form an expression for the equilibrium curve in Figure 1b.

$$y^i = \frac{\alpha_{ij} x_i}{1 + (\alpha_{ij} - 1)x_i} \tag{2a}$$

The relative volatility, α, is a direct measure of the ease of separation by distillation. If $\alpha = 1$, then component separation is impossible, because the liquid- and vapor-phase compositions are identical. Separation by distillation becomes easier as the value of the relative volatility becomes increasingly greater than unity. Distillation separations having α values less than 1.2 are relatively difficult; those that have values above 2 are relatively easy.

When both phases form ideal thermodynamic solutions, ie, no heat of mixing, no volume change on mixing, etc, Raoult's law applies:

$$p_i{}^V = x_i P_i{}^0 \tag{3}$$

where $P_i{}^0$ is the vapor pressure of i at the equilibrium temperature. Combining this expression with Dalton's law of partial pressures, K values and relative volatilities may be obtained:

$$K_i = P_i{}^0/P \tag{4}$$

$$\alpha_{ij} = P_i{}^0/P_j{}^0 \tag{5}$$

Examples of ideal binary systems are benzene–toluene and ethylbenzene–styrene; the molecules are similar and within the same chemical families. Thermodynamics texts should be consulted before making the assumption that a chosen binary or multicomponent system is ideal. When pressures are low and temperatures are at ambient or above, but the solutions are not ideal, ie, there are dissimilar molecules, corrections to equations 4 and 5 may be made:

$$K_i = \gamma_i{}^L P_i{}^0/P \tag{6}$$

$$\alpha_{ij} = \gamma_i{}^L P_i{}^0/(\gamma_j{}^L P_j{}^0) \tag{7}$$

where the Raoult's law correction factor, γ^L, is a thermodynamically important liquid-phase activity coefficient.

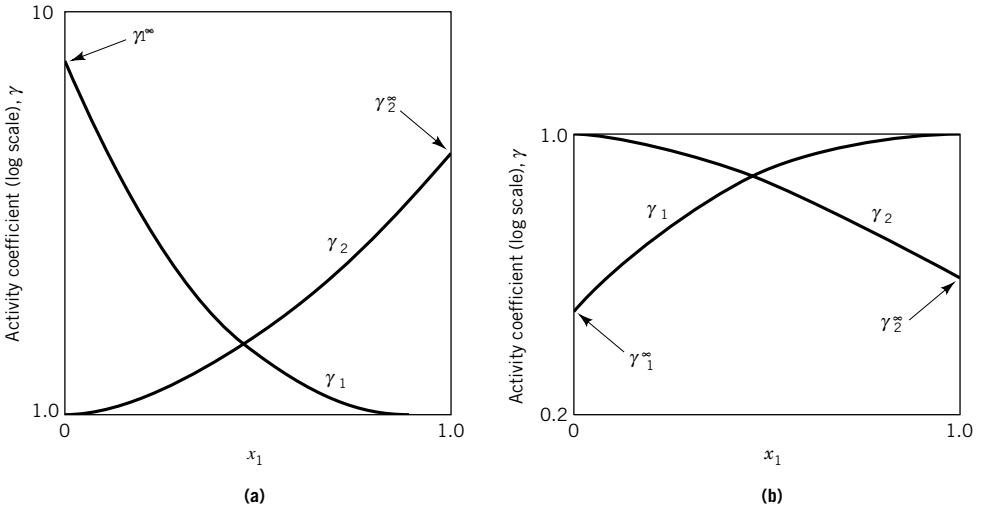

Fig. 3. Binary activity coefficients for two component systems having (**a**) positive and (**b**) negative deviations from Raoult's law. Conditions are either constant pressure or constant temperature and terminal coefficients, γ_i^∞, are noted.

The development and thermodynamic significance of activity coefficients is discussed in most chemical engineering thermodynamics texts. The liquid-phase coefficients are strong functions of liquid composition and temperature and, to a lesser degree, of pressure. A system with positive deviation, ie, the two components having activity coefficients greater than one such that the logarithm of the coefficient is positive, is shown in Figure 3**a**; a system with negative deviation, the coefficients are less than unity and logarithms negative, is shown in Figure 3**b**. In a few cases one component of a binary mixture has a positive deviation and the other a negative deviation. Most commonly, however, both coefficients have positive deviations.

Terminal activity coefficients, γ_i^∞, are noted in Figure 3. These are often called *infinite dilution coefficients* and for some systems are given in Table 1.

Table 1. **Terminal Activity Coefficients at Atmospheric Pressure**[a]

Component 1	Component 2	γ_1^∞	γ_2^∞
chloroform	ethyl acetate	0.3	0.3
chloroform	benzene	0.9	0.7
n-hexane	*n*-heptane	1.0	1.0
ethyl acetate	ethanol	2.5	2.5
ethanol	toluene	6.0	6.0
benzene	methanol	9.0	9.0
ethanol	isooctane	11.0	8.0
methyl acetate	water	20.0	7.0
ethyl acetate	water	100.0	15.0
hexane	water	>100.0	>100.0

[a] Values are approximate.

The hexane–heptane mixture is included as an example of an ideal system. As the molecular species become more dissimilar, they are prone to repel each other, tend toward liquid immiscibility, and have large positive activity coefficients, as in the case of hexane–water.

If the molecular species in the liquid tend to form complexes, the system will have negative deviations and activity coefficients less than unity, eg, the system chloroform–ethyl acetate. In azeotropic and extractive distillation (see DISTILLATION, AZEOTROPIC AND EXTRACTIVE) and in liquid–liquid extraction, nonideal liquid behavior is used to enhance component separation (see EXTRACTION, LIQUID–LIQUID). An extensive discussion on the selection of nonideal addition agents is available (17).

A great deal of study and research has gone into the development of working equations that can represent the curves of Figure 3. These equations are based on solutions of the Gibbs-Duhem equation:

$$x_i \left[\frac{\alpha \ln \gamma_i}{\alpha x_i}\right]_{T,P} + \cdots x_n \left[\frac{\alpha \ln \gamma_n}{\alpha x_i}\right]_{T,P} = 0 \tag{8}$$

One of the simplest and often used equations, or models, is that of Van Laar (18). For a binary system of components 1 and 2, these equations are

$$\ln\gamma = \frac{A_{12}}{\left[1 - \frac{A_{12}x_1}{A_{21}x_2}\right]^2} \tag{9}$$

$$\ln\gamma_2 = \frac{A_{21}}{\left[1 - \frac{A_{21}x_2}{A_{12}x_1}\right]^2} \tag{10}$$

It should be noted that only two parameters are involved. They are directly related to the terminal activity coefficients:

$$\ln \gamma_1^\infty = A_{12} \tag{11}$$

$$\ln \gamma_2^\infty = A_{21} \tag{12}$$

A useful and quite popular model is given (19):

$$\ln \gamma_1 = -\ln(x_1 + \Lambda_{12}x_2) + \left(\frac{\Lambda_{12}}{x_1 + \Lambda_{12}x_2} - \frac{\Lambda_{21}}{\Lambda_{21}x_1 + x_2}\right) \tag{13}$$

$$\ln \gamma_2 = -\ln(x_2 + \Lambda_{21}x_1) - \left(\frac{\Lambda_{12}}{x_1 + \Lambda_{12}x_2} - \frac{\Lambda_{21}}{\Lambda_{21}x_1 + x_2}\right) \tag{14}$$

This, the Wilson model, is more complex than the Van Laar model, but it does retain the two-parameter feature. The terminal activity coefficients are related to the parameters:

$$\ln \gamma_1^{\infty} = 1 - \ln \Lambda_{12} - \Lambda_{21} \tag{15}$$

$$\ln \gamma_1^{\infty} = 1 - \ln \Lambda_{21} - \Lambda_{12} \tag{16}$$

Whereas the Wilson model has been found to represent a wide variety of nonideal VLE, it cannot handle the case of partial immiscibility of the liquid phase; for this purpose a three-parameter relationship, the nonrandom, two-liquid (NRTL) model was developed (20).

The most recently developed model is called UNIQUAC (21). Comparisons of measured VLE and predicted values from the Van Laar (22), Wilson, NRTL, and UNIQUAC models, as well as an older model, are available (3). Thousands of comparisons have been made, and Reference 3, which covers the Dortmund Data Base, available for purchase and use with standard computers, should be consulted by anyone considering the measurement or prediction of VLE. The predictive VLE models can be accommodated to multicomponent systems through the use of certain combining rules. These rules require the determination of parameters for all possible binary pairs in the multicomponent mixture. It is possible to use more than one model in determining binary pair data for a given mixture (23).

To estimate VLE when no experimental data or model parameters are available and the cost of special measurements cannot be justified, a group contribution method based on the molecular structures involved called UNIFAC (8) has been developed. Not all possible groups have been evaluated, but regular progress reports are published. The UNIFAC method, as well as the other models, are critically important in extending limited data to conditions in distillation columns that can cover wide ranges of temperatures, pressures, and compositions. Handling of all these models by computer solution has been described in some detail (24) (see also ENGINEERING, CHEMICAL DATA CORRELATIONS).

The vapor–liquid equilibria of dilute solutions are frequently expressed in terms of Henry's law:

$$p_i{}^V = H_i{}^* x_i \tag{17}$$

where, From equation 6, the Henry's law coefficient is

$$H_i{}^* = \gamma_i{}^L P_i{}^0 \tag{18}$$

Henry's law is useful for handling equilibria associated with gas absorption (qv) and stripping problems. Henry's law coefficients are useful for estimating terminal activity coefficients and have been tabulated for many compounds in dilute aqueous solutions (25,26).

The foregoing discussion has dealt with nonidealities in the liquid phase under conditions where the vapor phase mixes ideally and where pressure–temperature effects do not result in deviations from the ideal gas law. Such

conditions are by far the most common in commercial distillation practice. However, it is appropriate here to set forth the completely rigorous thermodynamic expression for the K value:

$$K_i = \frac{\gamma_i^L \phi_i^0 p_i^0 \exp\left(\frac{1}{R'T}\int_{p_i^0}^{p} v_i^L \, dP\right)}{\hat{\phi}_i P} \tag{19}$$

For nonideal vapor-phase behavior, the fugacity coefficient for component i in the mixture must be determined:

$$\ln \hat{\phi}_1 = \frac{1}{R'T}\int_0^P \left(v_i^v - \frac{R'T}{P}\right) dP \tag{20}$$

If the vapor forms an ideal solution,

$$v_i^v = v^v = zR'T/P \tag{21}$$

where z is the compressibility factor for the mixture. The right side of the numerator in Equation 19 is called the Poynting correction, PC:

$$PC = \exp\left(\frac{1}{R'T}\int_{p_i^0}^{p} v_i^L \, dP\right) \tag{22}$$

when the liquid is incompressible,

$$PC = \exp\left(\frac{v_i^L (P - P_i^0)}{R'T}\right) \tag{23}$$

At pressures less than 2 MPa (20 bar) and temperatures greater than 273 K, $PC \sim 1.0$. When the vapor obeys the ideal gas law, $z = 1.0$; then for ideal vapor solutions and for conditions such that $PC = 1.0$, Equation 19 reduces to Equation 6.

The fugacity coefficient departure from nonideality in the vapor phase can be evaluated from equations of state or, for approximate work, from fugacity/compressibility estimation charts. References 11,14, and 25 provide valuable insights into this matter.

Journals for the publication of VLE data are available as are comprehensive tabulations of azeotropic data (27,28); if the composition and temperature of the azeotrope are known (at a given pressure), then such information may be used to calculate activity coefficients. At the azeotropic point, by definition, $y_i = x_i$; from Equation 6,

$$\gamma_i{}^L = P/P_i{}^0 \tag{24}$$

The vapor pressure $P_i{}^0$ can be obtained from any of many sources such as handbooks.

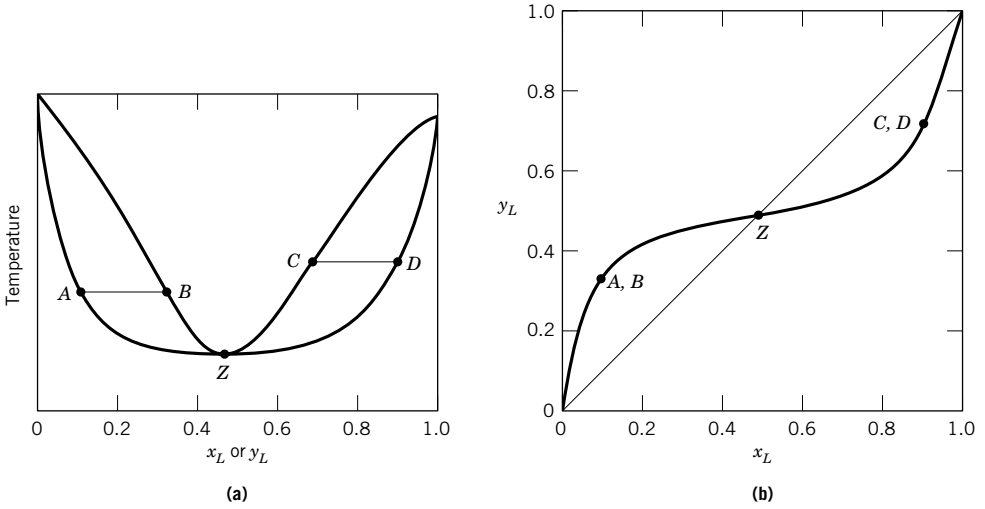

Fig. 4. Boiling point (**a**) and phase diagram (**b**) for a minimum boiling binary azeotropic system at constant pressure. *A,B* and *C,D* are representative equilibrium points; *Z* is the azeotropic point.

The measurement of VLE can be carried out in several ways. A common procedure is to use a recycle still, which is designed to ensure equilibrium between the phases. Samples are then taken and analyzed by suitable methods. It is possible in some cases to extract equilibrium data from chromatographic procedures. Discussions of experimental methods are available (5,11). For the more challenging measurements, eg, conditions where one or more components in the mixture can decompose or polymerize, commercial laboratories can be used.

2.2. Azeotropic Systems. An azeotropic mixture is one that vaporizes without any change in composition. Figures 4 and 5 represent homogeneous azeotropic systems. Figure 4 depicts a minimum boiling azeotropic system such as ethanol–water; Figure 5 describes a maximum boiling azeotropic system such as acetone–chloroform. The point *Z* defines the azeotropic composition; this azeotropic mixture is also called the constant boiling mixture (CBM). Positive activity coefficients tend to produce minimum boiling azeotropes, and negative coefficients tend to produce maximum boiling azeotropes.

Heterogeneous azeotropes are formed when the positive activity coefficients are sufficiently large to produce two liquid phases that exist at the boiling point, and a constant boiling mixture that is formed at some composition, generally within the liquid immiscibility composition range. An example of a heterogeneous azeotropic system is the water/1-butanol system shown in Figure 6. Within the immiscible range, *M–N*, the equilibrium vapor is the heterogeneous azeotrope, *Z*, of constant composition and the equilibrium temperature is constant. At liquid compositions lower in water than in the azeotrope, the relative volatility of water/1-butanol is greater than one; at liquid compositions higher in water than in the azeotrope, the relative volatility of water/1-butanol is less than one (see DISTILLATION, AZEOTROPIC AND EXTRACTIVE).

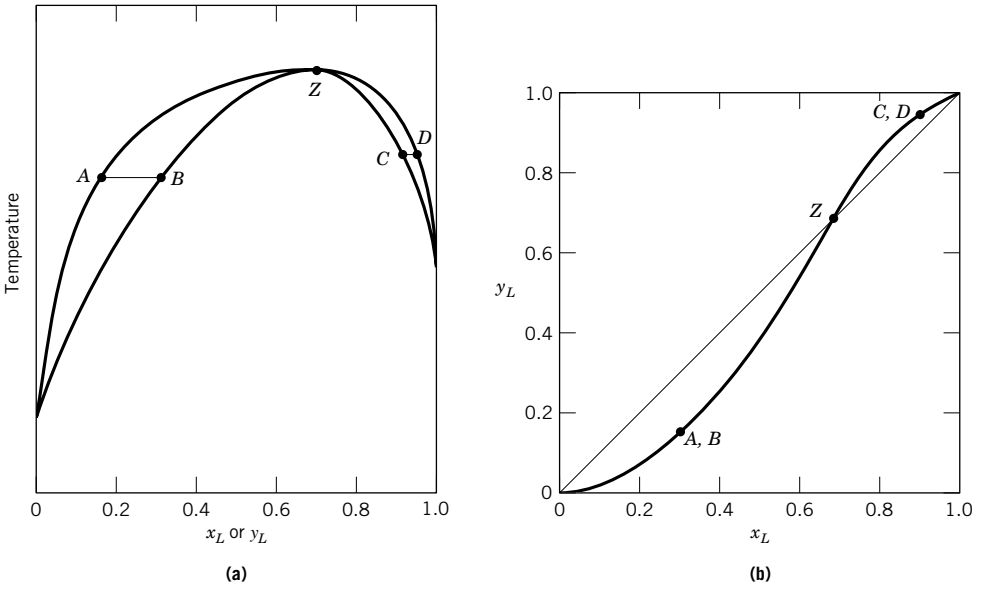

Fig. 5. Boiling point (**a**) and phase diagram (**b**) for a maximum boiling binary azeotropic system at constant pressure. *A,B* and *C,D* are representative equilibrium points; *Z* is the azeotropic point.

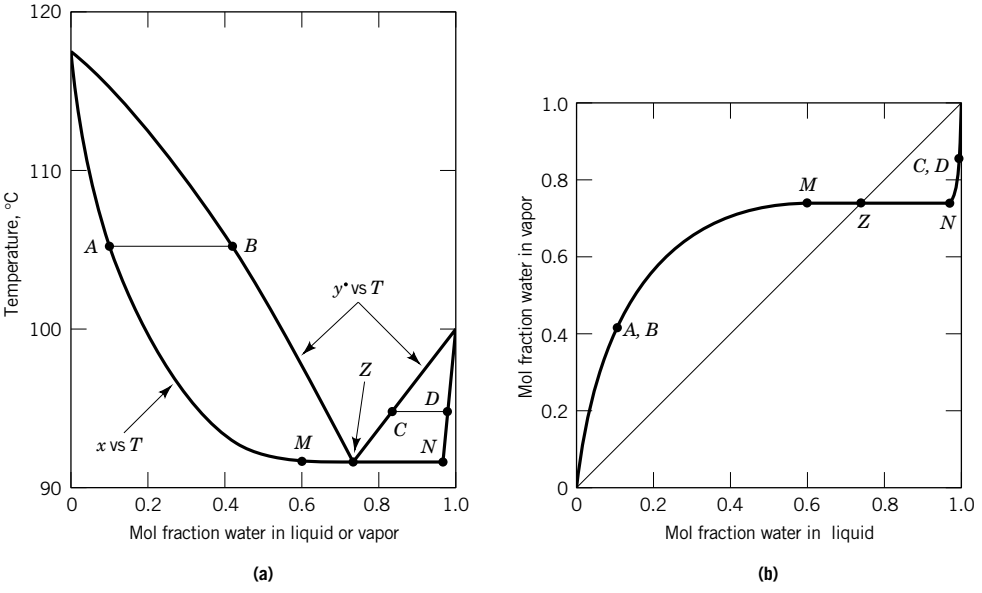

Fig. 6. Boiling point (**a**) and phase diagram (**b**) for the heterogeneous azeotropic system, water/1-butanol at atmospheric pressure. *A,B* and *C,D* are representative equilibrium points; *Z* is the azeotropic point; *M* and *N* are liquid miscibility limits.

3. Distillation Processes

Basic distillation involves application of heat to a liquid mixture, vaporization of part of the mixture, and removal of the heat from the vaporized portion. The resultant condensed liquid, the distillate, is richer in the more volatile components and the residual unvaporized bottoms are richer in the less volatile components. Most commercial distillations involve some form of multiple staging in order to obtain a greater enrichment than is possible by a single vaporization and condensation.

For ease of presentation and understanding, the initial discussion of distillation processes involves binary systems. Examining the binary boiling point (Fig. 1**a**) and phase (Fig. 1**b**) diagrams, the enrichment from liquid composition x_L to vapor composition y_L represents a theoretical step, or equilibrium stage.

3.1. Simple Distillations. Simple distillations utilize a single equilibrium stage to obtain separation. Simple distillation, also called differential distillation, may be either batch or continuous, and may be represented on boiling point or phase diagrams. In Figure 1a, if the batch distillation begins with a liquid of composition x_L^A the initial distillate vapor composition is y_L^A. As the distillate is removed, the remaining liquid becomes less rich in the low boiler, L, and the boiling liquid composition moves to the left along the bubble point line. If the distillation is continued until the liquid has a composition of x_L^E, the last vapor distillate has a composition of y_L^E. Simple batch distillation is not widely used in industry, except for the processing of high-valued chemicals in small production quantities, or for distillations requiring regular sanitization. Calculation methods are found in most standard distillation texts, and as parts of commercial process simulation computer software packages.

Simple continuous distillation, also called flash distillation, has a continuous feed to a single equilibrium stage; the liquid and vapor leaving the stage are considered to be in phase equilibrium. On the boiling point diagram (Fig. 1a), the feed is represented by x_L^F, the bottoms liquid by x_L^B, and the equilibrium vapor distillate by y_L^D. The overall mass balance is

$$F = D + B \tag{25}$$

the component L balance is

$$x_L{}^F F = y_L{}^D D + x_L{}^B B \tag{26}$$

Flash distillations are widely used where a crude separation is adequate. Examples of flash multicomponent calculations are given in standard distillation texts (29).

3.2. Multiple Equilibrium Staging. The component separation in simple distillation is limited to the composition difference between liquid and vapor in phase equilibrium. To overcome this limitation, multiple equilibrium staging is used to increase the component separation. Figure 7 schematically represents a continuous distillation that employs multiple equilibrium stages stacked one upon another. The feed, F, enters the column at equilibrium stage f. The heat q^s required for vaporization is added at the base of the column in a reboiler or

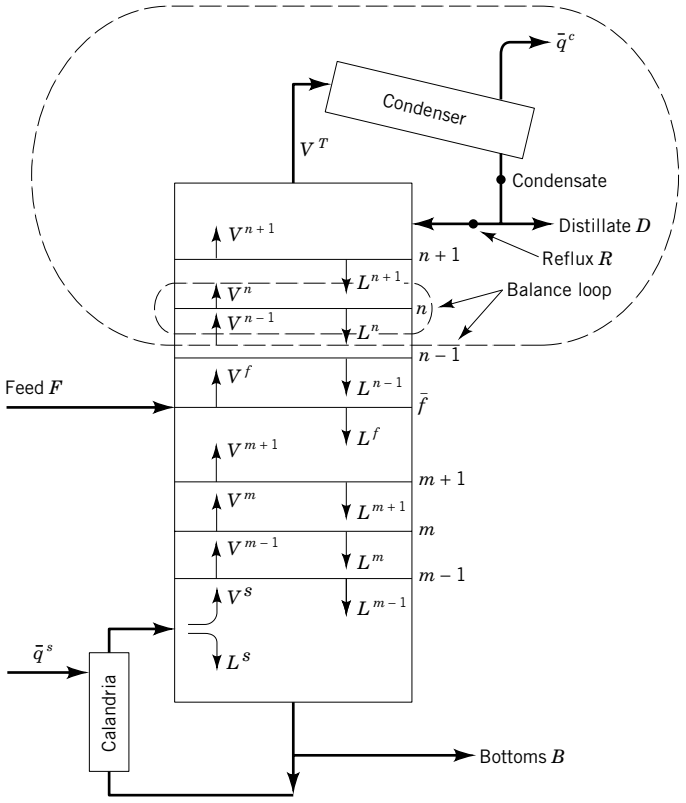

Fig. 7. Distillation column with stacked multiple equilibrium stages. Terms are defined in text.

calandria. The vapors V^T from the top of the column flow to a condenser from which heat q^c is removed. The liquid condensate from the condenser is divided into two streams: the first, a distillate D, which is the overhead product (sometimes called heads or make), is withdrawn from the system, and the second, a reflux R, which is returned to the top of the column. A bottoms stream B is withdrawn from the reboiler. The overall separation is represented by feed F separating into a distillate D and a bottoms B.

Above the feed a typical equilibrium stage is designated as n; the stage above n is $n+1$ and the stage below n is $n-1$. The section of column above the feed is called the *rectification section* and the section below the feed is referred to as the *stripping section*.

The mass balance across stage n is (*1*) vapor (V^{n-1}) from the stage below ($n-1$) flows up to stage n; (*2*) liquid (L^{n+1}) from the stage above ($n+1$) flows down to stage n; (*3*) on stage n the vapors leaving V^n are in equilibrium with the liquid leaving L^n. The vapors moving up the column from equilibrium stage to equilibrium stage are increasingly enriched in the more volatile components. Similarly, the liquid streams moving down the column are increasingly diminished in the more volatile components.

The overall column mass balances are

$$F = D + B \tag{27}$$

and for any component i,

$$Fx_i^F = Dx_i^D + Bx_i^B \tag{28}$$

The overall enthalpy balance is

$$H^F F + H^S = H^D D + H^B B + H^C \tag{29}$$

A mass balance around plate n and the top of the column gives:

$$V^{n-1} = L^n + D \tag{30}$$

And for any component:

$$V^{n-1} y_i^{n-1} = L^n x_i^n + D x_i^D \tag{31}$$

$$y_i^{n-1} = \left(\frac{L^n}{V^{n-1}}\right) x_i^n + \left(\frac{D}{V^{n-1}}\right) x_i^D \tag{32}$$

Below the feed, a similar balance around plate m and the bottom of the column results in:

$$y_i^{m-1} = \left(\frac{L^m}{V^{m-1}}\right) x_i^m + \left(\frac{B}{V^{m-1}}\right) x_i^B \tag{33}$$

Equation 32 represents the upper (or rectifying) operating line equation, and Equation 33 represents the lower (or stripping) operating line equation. The slopes L^n/V^{n-1} and L^m/V^{m-1} can vary, depending on heat effects.

Graphical Method. The graphical McCabe–Thiele (30) design method facilitates a visualization of distillation principles while providing a solution to the material balance and equilibrium relationships. Here, the subscripts L and H are not used, and x and y refer to the lower boiler, ie, more volatile component, in the binary system. A McCabe–Thiele diagram is given in Figure 8 where P, Q, and S are the x^B, x^F, and x^D compositions on the $y = x$, 45° construction line, respectively. Line OP is the stripping operating line and line OS is the rectifying operating line.

The McCabe–Thiele method employs the simplifying assumption that the molal overflows in the stripping and the rectification sections are constant. This assumption reduces the rectifying and stripping operating line equations to:

$$y^{n-1} = \left[\frac{\bar{L}}{\bar{V}}\right]_R x^n + \left(\frac{D}{\bar{V}_R}\right) x^D \tag{34}$$

$$y^{m-1} = \left[\frac{\bar{L}}{\bar{V}}\right]_S x^m + \left(\frac{B}{\bar{V}_S}\right) x^B \tag{35}$$

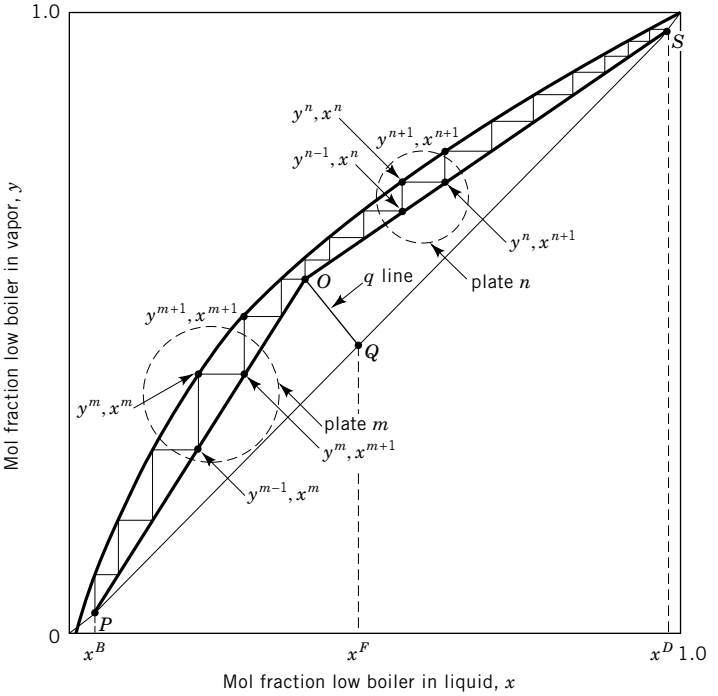

Fig. 8. McCabe–Thiele diagram. Terms are defined in text.

The constant molal flows in each section are designated by L and V. The McCabe–Thiele assumption of constant molal overflow implies that the molal latent heats of the two components are identical, the sensible heat effects are negligible, and the heat of mixing and the heat losses are zero. This simplified situation is closely approximated for many distillations. Equation 34 now represents the straight upper operating line OS, and Equation 35 represents the straight lower operating line OP. The upper operating line has the slope $(L/V)_R$ and the intercept at x^D $(= y^D)$ on the $x = y$ line. Note that this operating line slope is less than one. Similarly, the lower operating line has a slope of $(L/V)_S$ and the intercept is at x^B on the $y = x$ line. This operating line has a slope greater than one. The line QO from the feed intercept Q to the intersection of the operating lines at O is called the q line.

The equilibrium curve gives the vapor–liquid relationships of y^n and x^n above the feed and of y^m and x^m below the feed. The upper operating line gives the relationship between y^{n-1} and x^n and the lower operating line gives the relationship y^{m-1} and x^m, ie, the streams passing each other. The graphical representation of theoretical equilibrium stages n and m is shown. The y^{m-1}, x^m to y^m, x^{L+1} represent the mass balance and phase equilibrium for theoretical stage m. Similarly, y^{n-1}, x^n to y^n, x^{n+1} represent theoretical stage n. The total number of theoretical stages in the column can now be stepped off starting either at the composition x^B and stepping upward or starting at x^D and stepping downward.

Condition of Feed (q Line). The q line, which marks the transition from rectifying to stripping operating lines, is determined by mass and enthalpy balances around the feed plate. These balances are detailed in distillation texts (15).

The slope of the q line is $q/(q-1)$ where:

$$q = \frac{\text{heat needed to vaporize one mole of feed}}{\text{molal latent heat of feed}} \tag{36}$$

The q line, therefore, depends on the enthalpy condition of the feed. Types of q lines are shown in Figure 9 and are listed below.

Feed enthalpy condition	q	Slope of q line	q Line coordinates
cold liquid	>1	+	Q–E
saturated liquid	1	∞	Q–D
partially vaporized	0–1	−	Q–C
saturated vapor	0	0	Q–B
superheated vapor	<0	+	Q–A

Reflux and Reflux Ratio. The liquid returned to the top of the column is called reflux. The molar ratio R/D is the external reflux ratio. The ratio $(L/\mathrm{V})_R$, which is the slope of the rectifying operating line, is the rectifying internal reflux ratio. Similarly, the ratio $(L/\mathrm{V})_S$, which is the slope of the stripping operating line, is the stripping internal reflux ratio. As the ratio R/D increases, the rectifying internal reflux ratio increases and numerically approaches unity; similarly,

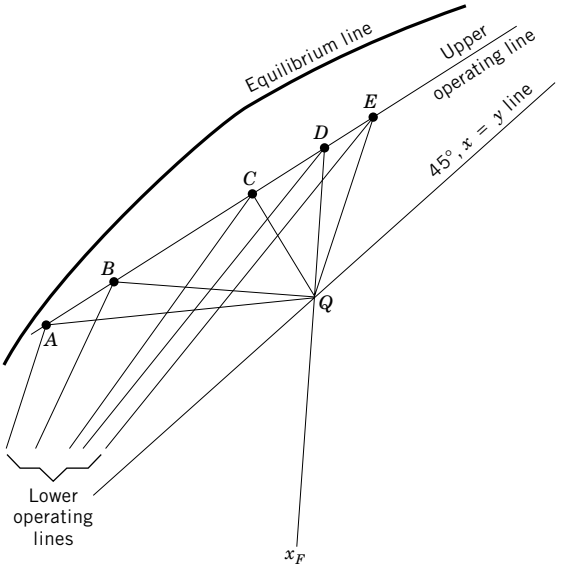

Fig. 9. McCabe–Thiele q lines for various feed enthalpy conditions. Terms are defined in text.

the stripping internal reflux ratio decreases and numerically approaches unity. In the McCabe–Thiele plot the two operating lines move away from the equilibrium line toward the $y = x$ diagonal as the reflux ratio increases, and the individual theoretical stage steps become larger; accordingly, fewer theoretical stages are required to make a given separation.

McCabe–Thiele Example. Assume a binary system L–H that has ideal vapor–liquid equilibria and a relative volatility of 2.0. The feed is 100 mol of $x^F = 0.6$; the required distillate is $x^D = 0.95$, and the bottoms $x^B = 0.05$, with the compositions identified and the lighter component L. The feed is at the boiling point. To calculate the minimum reflux ratio, the minimum number of theoretical stages, the operating reflux ratio, and the number of theoretical stages, assume the operating reflux ratio is 1.5 times the minimum reflux ratio and there is no subcooling of the reflux stream, then:

(*1*) Calculate the vapor composition in equilibrium with the liquid feed. From Equation 2a and for $x = 0.60$ mol fraction;

$$y^* = \frac{2(0.6)}{1 + (2.0 - 1)0.6} = 0.75 \text{ mol fraction} \tag{37}$$

(*2*) Similarly, the entire equilibrium curve is calculated and is plotted in Figure 10. The feed is at the boiling point so the q line is drawn vertically with an infinite slope.

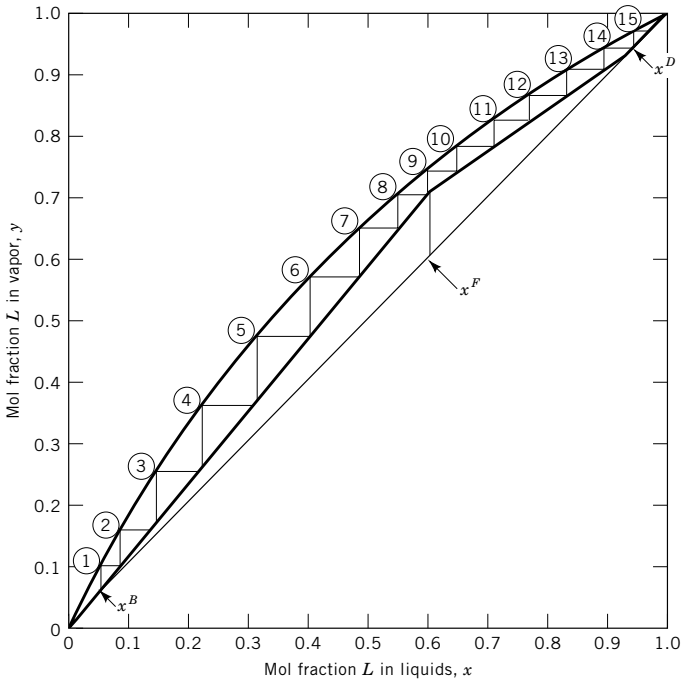

Fig. 10. McCabe–Thiele example. See text.

(*3*) Calculate mass balances on the basis of 100 mol of feed:

$$F = D + B \text{ (overall column balance)}$$

$$0.60F = 0.95D + 0.05B = 60 \text{ (component } L \text{ balance)}$$

$$D = 61.11 \text{ mol distillate}$$

$$B = 38.89 \text{ mol bottoms}$$

(*4*) Calculate reflux ratios. The minimum internal reflux ratio is a line from the intercept of the q line with the equilibrium curve to the x^D point on the 45° line:

$$\text{slope} = (L/V)_R = (0.95 - 0.75)/(0.95 - 0.60)$$

$$= 0.5714 \text{ minimum internal reflux ratio}$$

$$V = L + D = 0.5714V + 61.11$$

$$V = 142.58 \text{ mol (at minimum reflux)}$$

$$L = 81.47 \text{ mol} = R \text{ (at minimum reflux)}$$

$$(R/D)_{\text{min}} = 81.47/61.11 = 1.333 \text{ (minimum reflux ratio)}$$

(*5*) Operating reflux ratio $= (R/D)_{\text{operating}} = 1.5 \times 1.333 = 2.0$.

(*6*) Reflux flow $= R = 2.0(61.11) = 122.22$ mol $= L$ (at operating reflux ratio).

(*7*) Rectifying section vapor flow $= V = L + D = 122.22 + 61.11 = 183.33$ mol.

(*8*) Upper operating line (eq. 34):

$$y^{n-1} = (122.22/183.33)x^n + (61.11/183.33)0.95 = 0.667x^n + 0.317$$

(*9*) Stripping section liquid and vapor flows, because the feed is at the boiling point,

$$L_S = L_R + F = 122.22 + 100 = 222.22 \text{ mol}$$

$$V_S = V_R = 183.33 \text{ mol}$$

(*10*) Lower operating line (eq. 35):

$$y^{m-1} = (222.22/183.33)x^m + (38.89/183.33)(0.05) = 1.212x^m - 0.0106$$

(*11*) Theoretical stages: the complete construction is shown in Figure 10. Stages were stepped off starting at the base. Approximately 14.2 theoretical

stages are required. This includes the reboiler, which normally functions as an equilibrium stage. Therefore, a capability of 13.2 theoretical stages in the column is needed. If the condenser were to condense only reflux, with the distillate product leaving the process as a vapor, it could be counted also as an equilibrium stage, making 12.2 stages needed for the column.

Unequal Molal Overflow. The McCabe–Thiele method is based on the simplifying assumption that the molal overflow is constant in both the rectifying and stripping sections. For many problems this assumption is not valid and more precise calculations are necessary. For the more general case, detailed enthalpy balances are made around individual stages or groups of stages. Standard distillation texts discuss the internal enthalpy calculations by algebraic balances or by graphical procedures; eg, Reference 15 details the stage-to-stage mass and enthalpy balances with equilibrium calculations and also by means of the graphical Ponchon–Savarit procedure (31,32). Hand algebraic and graphical methods requiring internal enthalpy calculations have been largely superseded by simulations performed on modern computing devices, including personal computers (see COMPUTER TECHNOLOGY).

Minimum Number of Theoretical Stages and Minimum Reflux Ratio. There are infinite combinations of reflux ratios and numbers of theoretical stages for any given distillation separation. The larger the reflux ratio, the fewer the theoretical stages required. For any distillation system with its given feed and its required distillate and bottoms compositions, there are two constraints within which the variables of reflux ratio and number of theoretical stages must lie: the minimum number of theoretical stages and the minimum reflux ratio. The minimum reflux ratio occurs when the reflux ratio is reduced so that the upper and lower operating lines and the q line are coincident at a single point on the equilibrium line as shown in Figure 11**a**. When this condition exists, an infinite number of theoretical stages would be required to make the separation. The

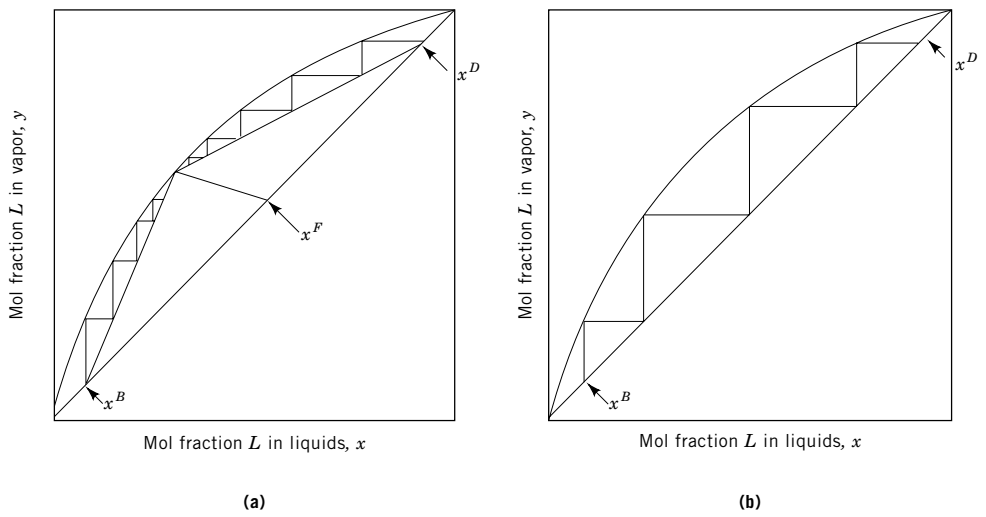

Fig. 11. Limiting conditions in binary distillation. (**a**) Minimum reflux and infinite number of theoretical stages; (**b**) total reflux and minimum number of theoretical stages.

minimum number of theoretical stages occurs when the system is at total reflux: no feed, distillate, or bottoms. This is illustrated in Figure 11**b**, where the operating lines are coincident with the 45°, $y = x$ line. For the McCabe–Thiele example presented above, the graphical procedure would give slightly less than nine minimum theoretical stages including the reboiler.

Simple analytical methods are available for determining minimum stages and minimum reflux ratio. Although developed for binary mixtures, they can often be applied to multicomponent mixtures if the two key components are used. These are the components between which the specification separation must be made; frequently the heavy key is the component with a maximum allowable composition in the distillate and the light key is the component with a maximum allowable specification in the bottoms. On this basis, minimum stages may be calculated by means of the Fenske relationship (33):

$$N_{\min} = \frac{\ln[(y_i/y_j)D(x_j/x_i)_B]}{\ln \alpha_{ij,\text{avg}}} \tag{38}$$

where i and j are the light and heavy components of a binary mixture, or the light key and heavy key in a multicomponent mixture. The average relative volatility is often taken as the geometric average of the relative volatilities at the top and bottom of the column. For the McCabe–Thiele example,

$$N_{\min} = \frac{\ln[(0.95/0.05)\,(0.95/0.05)]}{\ln 2.0} = 8.50 \text{ stages}$$

For minimum reflux ratio, the following equations (35) may be used:

$$\sum_i \frac{\alpha_i x_{if}}{\alpha_i - \phi} = 1 - q \tag{39}$$

$$\sum_i \frac{\alpha_i (x_{id})}{\alpha_i - \phi} = R_{\min} + 1 \tag{40}$$

where the value of q is determined as in the McCabe–Thiele procedure. Equation 39 is solved for root ϕ, the value of which must lie between 1.0 and the light key volatility. The root value so determined is then used in equation 40 to obtain the value of $R_{\min}$. Although a trivial example, the McCabe–Thiele problem would yield

$$\frac{2.0(0.6)}{2.0 - \phi} + \frac{1.0(0.4)}{1.0 - \phi} = 1 - q = 0 \text{ (because } q = 1)$$

solving $\phi = 1.25$. Substituting in equation 40, for the given distillate compositions,

$$\frac{2.0(0.95)}{2.0 - 1.25} + \frac{1.0(0.05)}{1.0 - 1.25} = R_{\min} + 1$$

from which $R_{\min} = 1.333$.

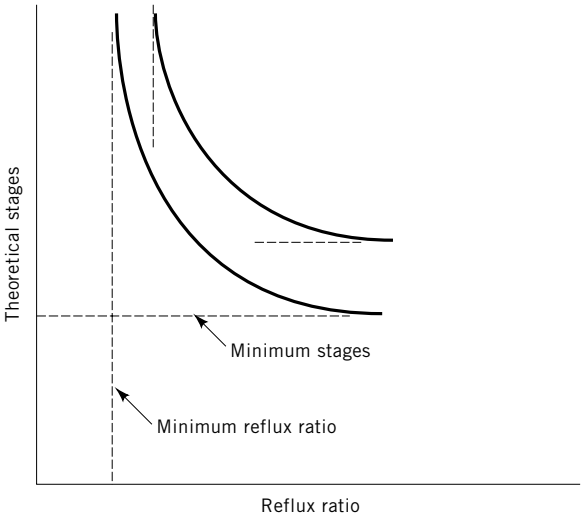

Fig. 12. Representative plot of theoretical stages vs reflux ratio for a given separation. Each curve is the locus of points for a given separation. Note the limiting conditions of minimum reflux and minimum stages.

Both of these limits, the minimum number of stages and the minimum reflux ratio, are impractical for useful operation, but they are valuable guidelines within which the practical distillation must lie. As the reflux ratio decreases toward the minimum reflux, the required number of stages increases rapidly. Similarly, as the minimum number of stages is approached, the required reflux ratio increases rapidly. A representative plot of the number of theoretical stages vs reflux ratio for some distillation separation is shown in Figure 12. Both minimum limits may be calculated for any distillation, thereby bracketing the practical design. Actual operating reflux ratios for most commercial columns are in the range of 1.1 to 1.5 times the minimum reflux ratio.

The operating, fixed, and total costs of a distillation system are functions of the relation of operating reflux ratio to minimum reflux ratio. Figure 13 shows a typical plot of costs; as the operating to minimum reflux ratio increases, the operating cost (principally energy cost for the boil-up) increases almost linearly. Similarly, the fixed costs at first decrease from the infinite number of stages, pass through a minimum, and then increase again as the diameter of column increases with increased reflux ratio. These costs for typical distillations have been calculated (36); the ratio of the economic optimum reflux to the minimum reflux is often 1.2 or less.

Minimum Reflux with Pinch Zone. There are some distillations where the minimum reflux does not occur at the intersection of the upper and lower operating lines and the q line. These cases arise when the equilibrium is skewed from positive activity coefficients and when the operating line intersects the equilibrium line in a zone of constant composition, a pinch zone, which is not at the q line intersection. Figure 14 illustrates such a case. An example of such a pinch zone in an ethanol–water column is available (36).

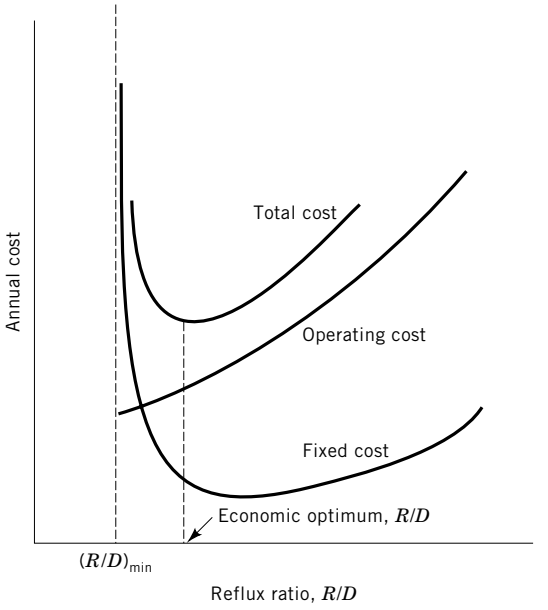

Fig. 13. Fixed, operating, and total costs of a typical distillation, as a function of reflux ratio.

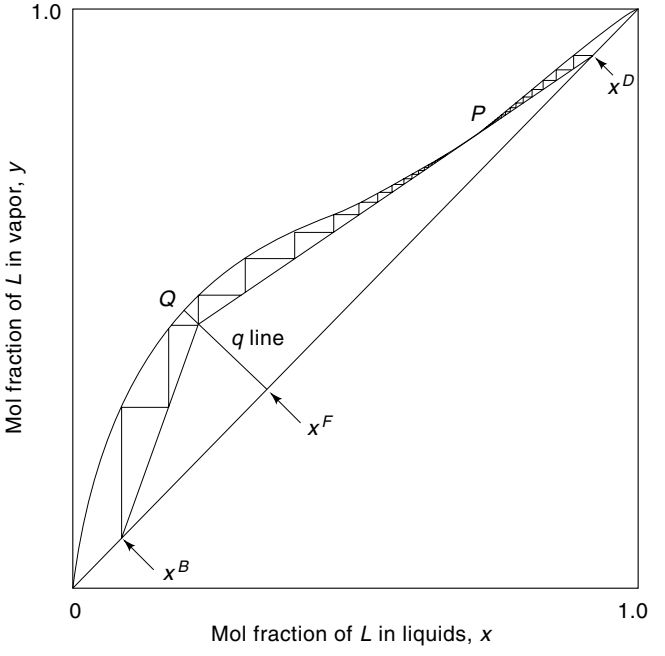

Fig. 14. False minimum reflux for system of skewed equilibria. Minimum reflux occurs at intersection P of operating line and equilibrium line, not at intersection of q line and equilibrium line. Terms are defined in text.

Multicomponent Calculations. The calculations that determine the reflux and stage requirements are more difficult to make for multicomponent systems than for binary systems. When the concentration of a component in the distillate and in the bottoms is specified for the overall solution of a binary distillation, the component balance around the column also is completely specified. In the multicomponent case, only a single high-boiling key component can be specified in the distillate and a single low-boiling key component in the bottoms; the split of other components can be determined only by detailed calculations. These require a series of trial and error computations to obtain the solution at any given reflux ratio and number of stages. As the number of components and number of stages become large, the mathematical problem becomes formidable. Two approaches may be followed: use of approximate, ie, shortcut, methods, or use of a suitable computer program that provides rigorous solutions. The former are used when approximate solutions are adequate or when a computer is not available. For the latter, numerous commercial programs are available and may be used with personal computers.

Most shortcut methods involve: (*1*) calculating the minimum number of stages; (*2*) calculating the minimum reflux ratio; and (*3*) estimating, from empirical correlations, the actual number of stages at an operating reflux. For minimum stages the Fenske relationship (eq. 38) is used, whereas for minimum reflux ratio the Underwood relationships (eqs. 39 and 40) are used. The relationship of operating to minimum reflux ratio and of operating to minimum number of plates is then estimated from the Gilliland correlation (37), or from a more recent correlation such as that of Reference 38.

The Gilliland correlation is in graphical form and the curve has been fitted by several workers, an example of which is (39):

$$\frac{N_t - N_{\min}}{N_t + 1} = 0.75 - 0.75\left[\frac{R - R_{\min}}{R + 1}\right]^{0.5668} \tag{41}$$

For the McCabe–Thiele example, and using eq. 41

$$\frac{N_t - 8.50}{N_t + 1} = 0.75 - 0.75\left[\frac{2.0 - 1.333}{2.0 + 1}\right]^{0.5668}$$

from which $N_t = 15.7$ stages. The original plot of Gilliland would give $N_t = 14.8$, closer to the McCabe–Thiele value of 14.2 stages.

Discussions of shortcut methods have appeared many times in the literature (16,35), accompanied by the usual admonition to use such methods only for approximate designs or analyses. For multicomponent systems having significant nonidealities, the shortcut methods can be grossly in error.

Rigorous computer solutions are used for complex distillations involving multiple stages, multiple components, nonideal phase equilibria, multiple feeds and drawoffs, and heat addition or removal at intermediate stages. Most calculations are made by computer and the algorithms are generally based on the Thiele–Geddes model (40), which rates a given number of stages and reflux

ratio for separation capability. A detailed discussion of computer solutions, including the handling of convergence problems, is available (41).

Computer solutions entail setting up component equilibrium and component mass and enthalpy balances around each theoretical stage and specifying the required design variables as well as solving the large number of simultaneous equations required. The explicit solution to these equations remains too complex for present methods. Studies to solve the mathematical problem by algorithm or iterational methods have been successful and, with a few exceptions, the most complex distillation problems can be solved.

3.3. Multiple Products. If each component of a multicomponent distillation is to be essentially pure when recovered, the number of columns required for the distillation system is N^*-1, where N^* is the number of components. Thus, in a five-component system, recovery of all five components as essentially pure products requires four separate columns. However, those four columns can be arranged in 14 different ways (42).

The number of columns in a multicomponent train can be reduced from the N^*-1 relationship if side-stream draw-offs are used for some of the component cuts. The feasibility of multicomponent separation by such draw-offs depends on side-stream purity requirements, feed compositions, and equilibrium relationships. In most cases, side-stream draw-off distillations are economically feasible only if component specifications for the side-stream are not tight. If a single component is to be recovered in an essentially pure state from a mixture containing both lower- and higher-boiling components, a minimum of two columns is required, one column to separate the lower boilers from the desired component and another column to separate the component from the higher boilers.

The economics of the various methods that are employed to sequence multicomponent columns have been studied. For example, the separation of three-, four-, and five-component mixtures has been considered (43) where the heuristics (rules of thumb) developed by earlier investigators were examined and an economic analysis of various methods of sequencing the columns was made. The study of sequencing of multicomponent columns is part of a broader field, process synthesis, which attempts to formalize and develop strategies for the optimum overall process (44) (see SEPARATION SYSTEMS SYNTHESIS).

4. Distillation Columns

Distillation columns are vertical, cylindrical vessels containing devices that provide intimate contacting of the rising vapor with the descending liquid. This contacting provides the opportunity for the two streams to achieve some approach to thermodynamic equilibrium. Depending on the type of internal devices used, the contacting may occur in discrete steps, called plates or trays, or in a continuous differential manner on the surface of a packing material. The fundamental requirement of the column is to provide efficient and economic contacting at a required mass-transfer rate. Individual column requirements vary from high vacuum to high pressure, from low to high liquid rates, from clean to dirty systems, and so on. As a result, a large variety of internal devices has been developed to fill these needs. The column devices discussed herein are

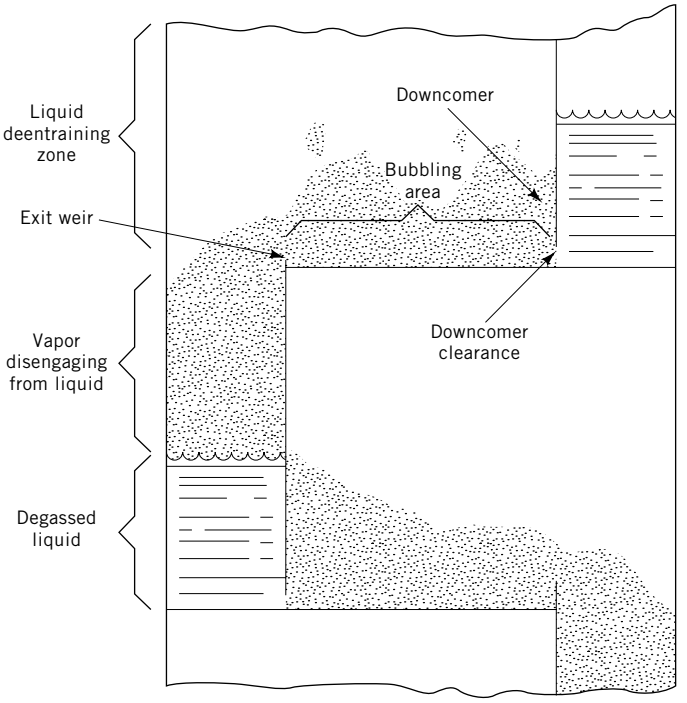

Fig. 15. Flow pattern in a crossflow plate distillation column.

used for absorption (qv) and stripping as well as distillation. The principal operational difference is that in absorption or stripping, the gas flowing up the column is primarily a noncondensable phase at column conditions, whereas in distillation the gas phase is a condensable vapor.

4.1. Plate Columns. There are two general types of plates in use: crossflow and counterflow. These names refer to the direction of the liquid flow relative to the rising vapor flow. On the cross-flow plate the liquid flows across the plate and from plate to plate via downcomers. On the counterflow plate liquid flows downward through the same orifices used by the rising vapor.

Crossflow Plates. As indicated in Figure 15, liquid enters a crossflow plate from the bottom of the downcomer of the plate above and flows across the active or bubbling area where it is aerated by the vapors flowing through orifices from the plate below. It is in this aerated zone where most of the vapor–liquid mass transfer occurs. The aerated mixture flows over the exit weir into a downcomer. A vapor–liquid disengagement takes place in the downcomer and most of the trapped vapor escapes from the liquid and flows back to the interplate vapor space. The liquid, essentially free of entrapped vapor, leaves the plate by flowing under the downcomer to the inlet side of the next lower plate. The vapor, disengaging from the aerated mass on the plate, rises to the next plate above.

The pressure drop incurred by the vapor as it passes through the orifices of the plate is fundamental to plate operation. In most plate designs, the pressure drop prevents the crossflowing liquid from falling through the plate. The pressure

drop also results from the energy consumed to disperse the vapor–liquid mixture, eg, to atomize a portion of the liquid to provide increased interfacial area for mass transfer. Diameters of commercial crossflow plate columns range from 0.3 to 15 m and plate spacings range from 0.15 to 1.2 m. The total pressure drop per plate is often in the range of 0.25–1.6 kPa (2–12 mm Hg).

Three principal vapor–liquid contacting devices are used in current crossflow plate design: the sieve plate, the valve plate, and a hybrid of the tow in which the "valves" are in a fixed, open position. In past years another type of crossflow plate containing bubble caps was specified, and there are some existing columns containing such vapor dispering devices. Details of the bubble cap tray and its design features were covered by Bolles (45). All the devices mentioned function to provide the needed intimate contacting of vapor and liquid, requisite to maximizing transfer of mass across the vapor–liquid interfacial boundary.

Sieve Plates. The conventional sieve or perforated plate is inexpensive and the simplest of the devices normally used. The contacting orifices in the conventional sieve plate are holes that measure 1 to 12 mm diameter and exhibit ratios of open area to active area ranging from 1:20 to 1:7. If the open area is too small, the pressure drop across the plate is excessive; if the open area is too large, the liquid weeps or dumps through the holes.

Valve Plates. Valve plates are categorized as proprietary and details of design vary from one vendor to another. These represent a variation of the sieve plate in which the holes are large and are fitted with liftable valve units such as those shown in Figure 16. The principal advantage over sieve plates is the ability to maintain efficient operation over a wider operating range through the use of variable orifices (valves), which open or close depending on vapor rate. The most common valve units consist of flat disks having attached legs that allow the valve to move upward or downward. Sometimes two weights of valves are used on a single plate to extend operating range and improve vapor distribution. The valve units usually have a tab or indentation that provides a minimum open area of vapor flow, even when the valve is closed, and also prevents the valve from sticking under corrosive or fouling conditions. Details on valve plate geometry, along with methods for valve plate design, are available from valve plate vendors.

Fixed Valve Plates. For several years plates with a combination of sieve holes and movable valves were marketed by several vendors, and can still be obtained on special order. Of more current interest is the crossflow tray containing

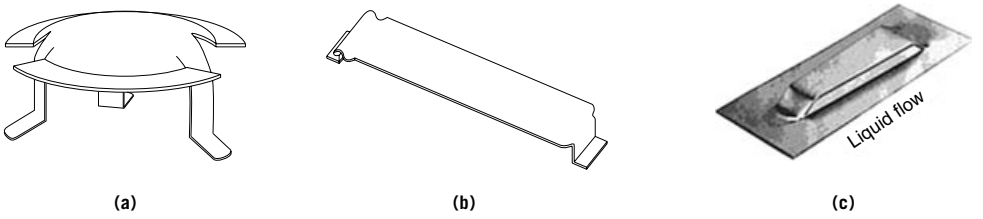

Fig. 16. Examples of individual valve units used in valve plates: (**a**) Flexitray valve, courtesy of Koch-Glitsch Inc.; (**b**) Float Valve, and (**c**) Fixed Valve (V-Grid), both courtesy of Sulzer Chem-Tech, Inc.

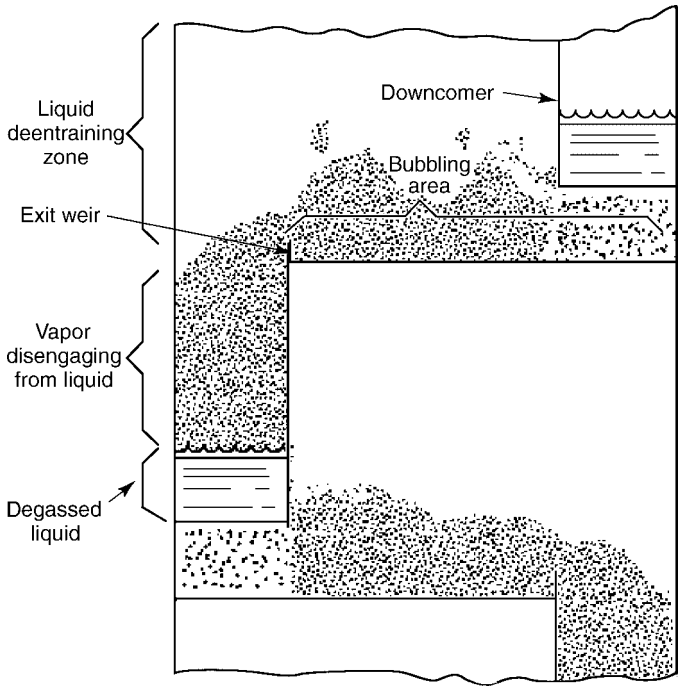

Fig. 17. Flow pattern in a high-capacity crossflow plate with suspended downcomer.

small "valves" that are fixed in the full open position. Some designers are specifing that the area under the downcomers be perforated with these fixed valves, requiring the downcomers to be suspended as shown in Figure 17. This arrangement allows an increase in vapor flow but requires careful design of the downcomer to prevent vapor by-passing up the downcomer.

Multiple Liquid-Path Plates. As the liquid flow rate increases in large diameter crossflow plates (ca 4 m or larger), the crest heads on the overflow weirs and the hydraulic gradient of the liquid flowing across the plate become excessive. To obtain improved overall plate performance, multiple liquid-flow-path plates may be used, with multiple downcomers. These designs are illustrated and discussed in detail in the literature (45).

Counterflow Plates. Counterflow plates are used less frequently than crossflow plates. The liquid flows downward and the vapor upward through the same orifices in a counterflow plate and the plate does not have downcomers. The openings are round holes (dualflow tray) or slots (Turbogrid tray). A variation of the dualflow tray is the Ripple tray in which the tray floor is shaped in a corrugated fashion (46). Counterflow plates are used advantageously in fouling services because for each hole vapor and liquid flow alternately, providing a self-cleaning action that is quite effective. The dualflow and Turbogrid plates have similar operating characteristics, and typical operating data have been published (47).

Another important plate which has characteristics similar to a counterflow plate is the Multiple Downcomer (MD) plate (48). This is a plate where the active

area occupies the full column cross section but with a plurality of small downcomers interspersed among the perforations. The downcomers are specially sealed to prevent upflow of vapor through them, as in the case of high-capacity suspended down comer plates (Fig. 17). The plate has been used successfully in many high-liquid-flow cases.

Vapor Capacity Parameters. The diameter of a distillation column is determined by the capacity of the column to handle the required flows of vapor and liquid. The vapor capacity parameter is

$$C_{sb} = V^* \left[\frac{\rho_g}{\rho_L - \rho_g} \right]^{0.5} \tag{42}$$

and its simplification

$$F^* = V^* \left(\rho_g \right)^{0.5} \tag{43}$$

The term C_{sb} in equation 42 is called a Souders–Brown capacity parameter and is based on the tendency of the upflowing vapor to entrain liquid with it to the plate above. The term F^* in equation 43 is called an F-factor. For C_{sb} and F^* to be meaningful the cross-sectional area to which they apply must be specified. The capacity parameter is usually based on the total column cross section minus the area blocked for vapor flow by the downcomer(s). For the F factor, typical operating ranges for sieve plate columns are

	Area basis	$(\text{kg}/(\text{m} \cdot \text{s}^2))^{0.5}$	$(\text{lb}/(\text{ft} \cdot \text{s}^2))^{0.5}$
$F_S{}^*$	total cross section	0.6–3.0	0.5–2.5
$F_A{}^*$	active area	0.85–4.3	0.7–3.5
$F_H{}^*$	hole area	8.5–30	7–25

Entrainment Flooding. The vapor capacity of a column is limited by excessive entrainment, usually called flooding. A flooding condition can be observed when the holdup of liquid becomes excessive, the pressure drop increases dramatically, and the mass-transfer efficiency falls precipitously. Estimates of the vapor velocity for a flooding condition may be made from the chart in Figure 18 (49). The abscissa term $L/\text{G}(\rho_g/\rho_L)^{0.5}$ is called a flow parameter and its value can indicate several things about the character of the aerated mass on the plate. For example, a very low value can indicate a phase inversion in which the vapor flow is continuous (spray flow), whereas a high value can indicate a bubbly mass (emulsion flow). The value of the flow parameter is easily determined from the stage calculations (reflux and boilup ratios) and densities of the phases. The ordinate value in Figure 18 leads to a value of the flooding velocity, and prudent design calls for limiting actual flows to 70–80% of this velocity.

Downcomer Flooding. For cases of very high liquid-to-vapor flow ratios the limiting capacity of the column is based on the ability of the downcomers to move the de-aerated liquid from a plate to the next plate below. It is clear

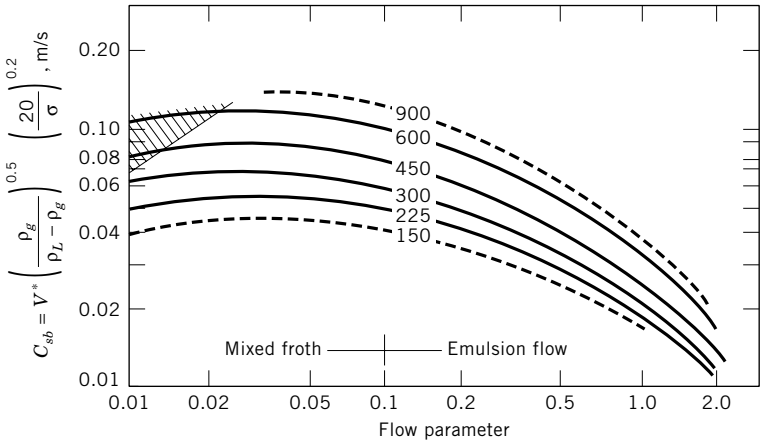

Fig. 18. Flooding correlation for crossflow trays (sieve, valve, bubble-cap) where the numbers represent tray spacing in mm. Also shown are approximate boundaries of the spray zone, and mixed froth and emulsion flow regimes.

that there can be constrictions in the downcomer design or that even with no constrictions there is simply not enough flow area to accommodate the high volume of liquid. Thus, the downcomer can flood, or choke, when it becomes completely filled with liquid or aerated mass. Typical design heuristics include limiting the downcomer velocity (clear liquid basis) to no more than 0.12 m/s. Also, to allow for complete disengagement of vapor from liquid in the downcomer, a minimum residence time of 4 s is often used. The actual limiting values of these parameters varies somewhat with the properties of the fluids and the exact dimensions of the plate components.

Stable Operating Range. All plates have a stable operating envelope bound by a range of liquid and vapor flow rates as shown in Figure 19. The size and shape of the stable area depends on the plate design and on the system properties. The line *AD* represents the minimum operable vapor flow rate at various liquid flow rates. Below *AD*, the vapor rate is too low to maintain the liquid on the plate and, as a result, the liquid weeps excessively or dumps through the plate orifices. Above line *BC* the column floods by entrainment. To the right of *CD* the high liquid rate causes downcomer flooding. The area to the left of *AB* represents high entrainment at low liquid flow rates, with vapor jets at the orifices. Design procedures for sieve plates have been published (eg 49,50). Vendors of valve trays make available their design methods.

Plate Efficiencies. Column requirements are calculated in terms of theoretical stages or plates. Actual plates must, however, be specified in the design. Thus the effectiveness of the plate in approaching the equilibrium condition must be predicted. This approach is called the plate efficiency, which is a measure of the rate of mass transfer on the actual plate. This efficiency, expressed either as a fraction or as a percentage, depends on three principal factors: the geometry of the plate (hole arrangement, valve design, etc); the loading of vapor and liquid traffic on the plate; and the diffusional properties of the fluids.

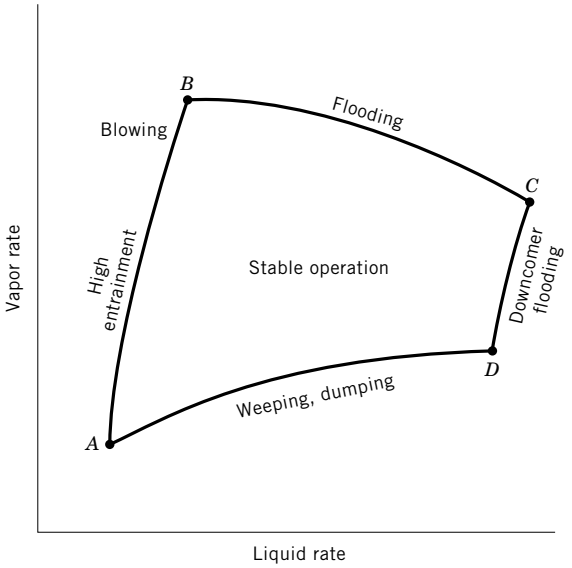

Fig. 19. Stable operating range for crossflow plates.

The simplest efficiency is the overall column efficiency, which is the number of theoretical plates in a column divided by the number of actual plates:

$$E_o = N_t/N_a \tag{44}$$

Thus the overall efficiency is an averaged efficiency of all the individual plates.

A more useful plate efficiency for theoretical prediction is the Murphree plate efficiency:

$$E_{mv} = \frac{y^n - y^{n-1}}{y^{n^*} - y^{n-1}} \tag{45}$$

where y^n and y^{n-1} are the vapor compositions from plate n and $n-1$ (the plate below n), and y^{n*} is the vapor composition that would be in equilibrium with the liquid composition leaving plate n. Thus, for a given plate, E_{mv} is a ratio of the actual vapor composition change to the change that would occur if the plate were effective enough to bring the vapor and liquid to thermodynamic equilibrium. This definition is based on the outlet liquid composition, and says nothing about the average liquid composition on the plate. In cases where a significant concentration gradient exists in the liquid composition across the plate, it is possible for E_{mv} to have a value greater than 1.0 (100%). Equation 45 is written in terms of vapor composition. A similar equation can be written in terms of the liquid compositions and is denoted as E_{mL}.

Of still more theoretical importance is the efficiency at some point on the plate:

$$E_{og} = \left[\frac{y^n - y^{n-1}}{y^{n^*} - y^{n-1}}\right]_{\text{point}} \tag{46}$$

This parameter is called the point efficiency (or local efficiency). It cannot have a value greater than 1.0, and it has a counterpart term for liquid compositions.

Prediction of Plate Efficiency. As of this writing, the most comprehensive study of plate efficiency known was made in the mid-1950s, based on the then-still-popular bubble cap plates (51). Unfortunately, the predictive model developed has been shown to be inadequate for many industrial distillations. An improvement of the model, more oriented toward the sieve plate, was published in 1984 (52). There has been continuing research effort directed toward a better understanding of the mechanisms that occur in the rather complex aerated mass on the typical plate (53–55). A complicating factor is the lack of uniform liquid flow across the plate, and situations have been found where the liquid actually stagnates in certain zones of larger-diameter plates. For larger columns it is possible for the observed Murphree efficiency to exceed 100%. A satisfactory method for predicting plate efficiency does not exist. Most recently there have been studies of the various types of flow regimes that occur on operating plates and of the effect of these regimes on tray performance, including plate efficiency. Pursuit of the flow regime studies (56–59) may lead to improved plate efficiency prediction methods. For example, a newer model (60) takes into account the regime as well as the vapor bubble (froth flow) or liquid drop (spray flow) characteristics in determining mass-transfer coefficients in the aerated zone on the plate.

Empirical methods for predicting plate efficiency have been proposed. Probably the most widely used method correlates overall column efficiency as a function of feed viscosity and relative volatility (61).

General Comments on Plate Efficiency. The plate efficiencies of well-designed commercial bubble cap, sieve, and valve plates are approximately the same when the plates are operated within their normal design range. The plate efficiency decreases both at the low end of the plate's operating range, where the liquid tends to leak through the plate, and at the high end of the operating range, where liquid entrainment becomes substantial.

Most distillation systems in commercial columns have Murphree plate efficiencies of 70% or higher. Lower efficiencies are found under system conditions of a high slope of the equilibrium curve (Fig. 1b), of high liquid viscosity, and of large molecules having characteristically low diffusion coefficients. Finally, most experimental efficiencies have been for binary systems where by definition the efficiency of one component is equal to that of the other component. For multicomponent systems it is possible for each component to have a different efficiency. Practice has been to use a pseudo-binary approach involving the two key components. However, a theory for multicomponent efficiency prediction have been developed (62,63) and are amenable to computational analysis.

4.2. Packed Columns. In packed columns, the vapor–liquid contacting takes place in continuous beds of solid packing elements rather than in discrete individual plates. The contacting can be visualized as occurring in differential increments across the height of the packing; thus packings are known as counterflow devices rather than stagewise devices. Mechanically, the packed column is a relatively simple structure. In its simplest form the packed column comprises a vertical shell having dumped or carefully arranged packing elements on an open-type support, together with a suitable liquid distribution device above the

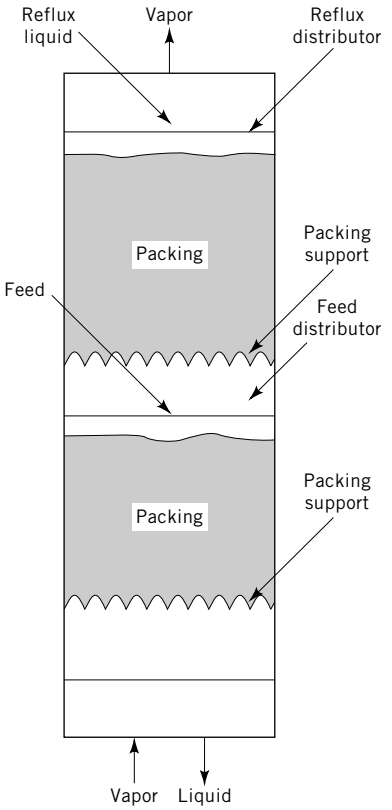

Fig. 20. Packed column shell and internals. Column shown has single packed beds above and below the feed. For separations requiring a large number of stages, additional beds, separated by redistribution devices, are likely to be needed.

packed bed. A packed column having two packed beds and a midcolumn feed is shown in Figure 20. The vapor enters the column below the bottom bed and flows upward through the column. The liquid (reflux or other liquid stream) enters at the top through the liquid distributor and flows downward through the packing counter-currently to the rising vapor. The height of the individual packed beds is limited to 2–9 m by the mechanical strength of the packing or by the need to redistribute the liquid so that good mass-transfer efficiency can be maintained.

Packings. For many years packed columns consisted of randomly dumped packings almost exclusively, with occasional applications of regularly stacked packings or pads of woven or knitted wire. In the late 1960s a partial trend away from random packings began when a special structured packing made of wire gauze was introduced by Sulzer Brothers in Switzerland (64). The indicated advantages of the structured packings were high mass-transfer efficiency and very low pressure drop. These devices appeared to be ideal for high-vacuum distillations. However, cost of fabrication was very high and they were considered mainly for the vacuum distillation of specialty chemicals. In 1977, a lower-cost sheet metal version was introduced (65), and since that time

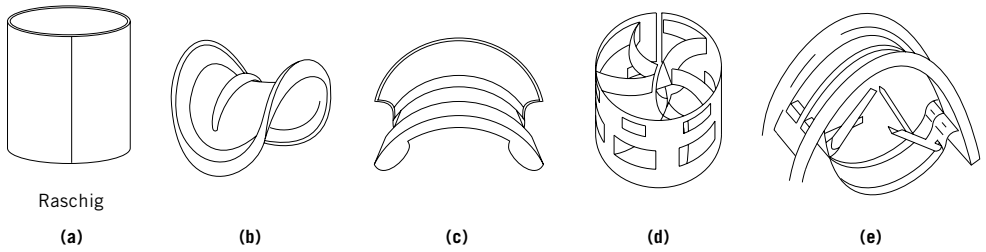

Fig. 21. Random packing elements for distillation columns: (**a**) Raschig ring (metal); (**b**) Berl saddle (ceramic); (**c**) Intalox saddle (ceramic); (**d**) Pall ring (metal); and (**e**) Intalox saddle (metal).

a large business in structured sheet metal packings has arisen. At the same time, improved random packings have been developed and a comprehensive discussion of their characteristics has been published (66). Some of the common random packings are shown in Figure 21. The Raschig ring, one of the oldest of packings, is an open cylinder of equal height and diameter. The Berl saddle and the ceramic Intalox saddle (Norton Co.) have a higher capacity and efficiency than the Raschig ring. The Pall ring is a modification of the Raschig ring which allows through-flow of liquid and vapor, with consequent lower pressure drop and better efficiency. The newer Intalox metal saddle (IMTP) is an example of a random packing having a very high void fraction and low resistance to the flowing phases. Other newer random packings, not shown in Figure 21, include the CMR ring (Koch-Glitsch, Inc.) and the Nutter ring (Sulzer Chemtech Inc.). The random-type packings can generally be made from metal, plastic, or ceramic materials; the approximate nominal size range for the individual elements is 12–75 mm.

Common structured packing geometries are shown in Figure 22. Flat plates of gauze or sheet metal are perforated, or embossed or lanced, and corrugated. Corrugated sheets are then stacked together such that adjacent sheets have opposite corrugation directions. The corrugations have angles with the horizontal of 45 to 60 degrees. Vapor and liquid contact each other in wetted-wall fashion, and the perforations plus other surface enhancements, eg, texturing, serve to promote liquid spreading into thin films. Dimensions, performance characteristics, and design procedures for the structured packings are summarized in Reference 67.

Packed Column Internals. In order to ensure good packed column mass-transfer efficiency, the liquid must be distributed uniformly over the surface of the packing. As a general rule there should be at least 100 pour points per square meter (10 points/ft^2), although fewer points may be used for random packings of the bluff-body type such as Raschig rings and Berl saddles. Although they have capacity and pressure drop limitations, the bluff-body packing elements are able to divide the downflowing liquid and thus improve on an initially marginal distribution. On the other hand, the through-flow-type random packings, eg, Pall rings and Intalox metal tower packings, as well as the structured packings, are not able to correct the initial distribution and in fact may allow some deterioration of distribution if the bed heights are greater than about 5 m.

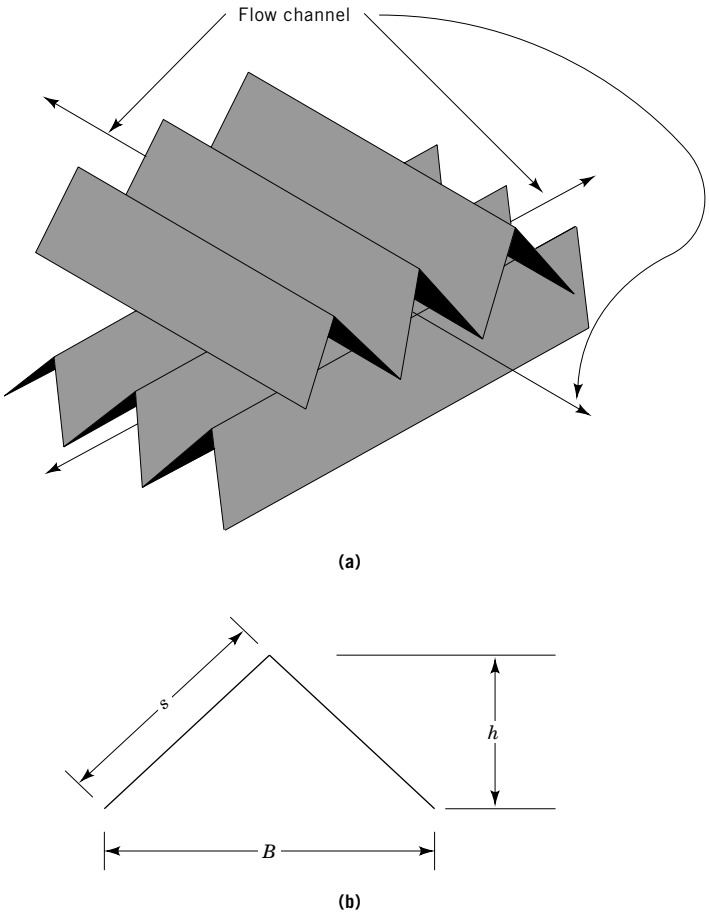

Fig. 22. (**a**) Flow channel arrangement; (**b**) flow channel triangular cross section where for angles of 90°, $D_{EQ} = 4R_H = 4(\frac{S}{2})\frac{1}{2S} = S$.

Considerable research is in progress on methods for ensuring good liquid distribution in large-diameter columns, and the packing manufacturers maintain large test stands where a particular design of distributor can be tested using water before being installed in the column. The distributor design problem becomes more severe at low, ie, $<700\ cm^3/(sm^2)\ (1\ gal/(min\ ft^2))$ liquid rates or in large (>3 m) diameter towers. An example of a more fundamental study of liquid distribution is available (68), as are typical liquid distributor designs and typical packing supports (50).

Packed Column Operation. In the packed column, liquid flows downward in opposition to the upward flow of vapor; both phases flow through the same open space or interstices between the packing elements. At low liquid and gas flow rates, the descending liquid occupies only a small fraction of the interstices and, therefore, offers little hindrance to the rising vapor flow. Figure 23 shows a schematic plot of pressure drop per unit of height as a function

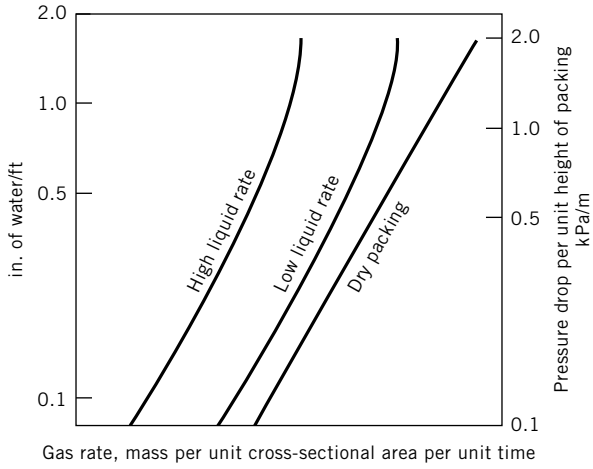

Fig. 23. Log–log plot of pressure drop per unit height of typical packing as a function of gas rate at two liquid rates and for the unirrigated packing.

of the gas rate at low and high liquid flow rates. At a low rate of gas flow, the log slope of each curve is approximately 2. As the gas flow rate increases, there is an increasing tendency for the liquid to be held up in the void space, thereby decreasing the space available for the gas flow. As the gas flow rate increases further, more liquid is held up until at some high gas rate the packing floods. At this point, the liquid is essentially filling the interstices and can no longer flow downward. At flooding, the log slope is practically infinite. The pressure drop at the inception of flooding ranges from 1.6 to 3.3 kPa/m (2 to 4 in. water/ft) of packing. More comprehensive discussions of packed column hydraulics may be found in distillation texts (15,17,69), monographs (66,70,71), or handbooks (72,73).

Capacity of Packed Columns. Packed columns are usually designed to operate at some percentage approach to flooding, eg, 60–70%, or at some specified pressure drop per unit height of packing, eg, 0.8 kPa/m (1 in. water/ft) of packing. Flooding correlations have been proposed (74), one revision introducing constant-pressure drop lines (75). The most recent revision in these correlations is shown in Figure 24 (66). The idea of flooding has been eliminated from the chart with the stipulation that the topmost curve represents the maximum capacity. Experimentally determined packing factors F_p, presented in Table 2, should be used in the ordinate group. These factors distinguish between the various shapes and sizes of the available packings. The curves are for constant pressure drop and thus the chart enables estimation of both capacity and pressure drop.

Packing Mass-Transfer Characteristics. The contacting for mass transfer in a packed column occurs differentially along the length of the column. The separation calculations can thus be made on a differential basis along this length, using mass-transfer coefficients or heights of transfer units. The calculations are somewhat imprecise because of the uncertainty in the fundamental

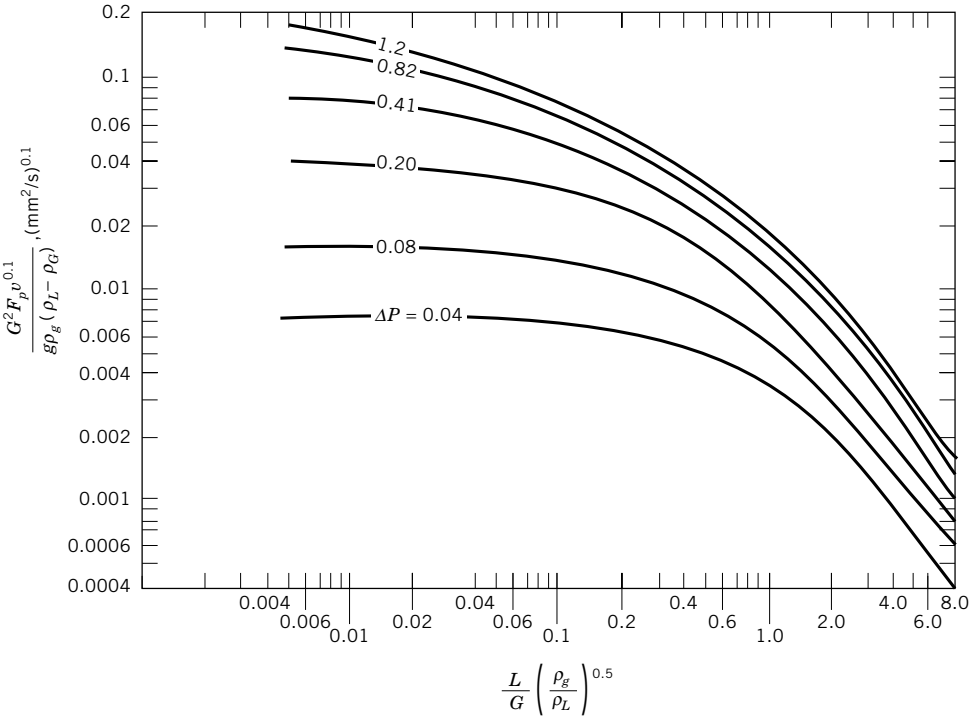

Fig. 24. Generalized method using log scales for estimating packed column flooding and pressure drop, ΔP, in kPa/m; g = gravitational constant, 9.81 m/s^2; v = kinematic viscosity in mm^2/s (= cSt); L, G have units of kg/(m^{2}s); ρ_L, ρ_G are in kg/m^3; and the packing factor, F_p, in m^{-1} can be found in Table 2. To convert kPa/m to mm Hg/m, multiply by 7.5 (66).

mass-transfer mechanisms in larger-scale columns. Useful models for predicting the mass-transfer efficiency of randomly packed columns have been published (76,77), using the same database of commercial-scale performance data. These models cover the better known packings, eg, metal and ceramic Raschig rings, ceramic Berl saddles, and metal Pall rings, in nominal sizes in the range of 12 to 50 mm. It has been found that to avoid excessive maldistribution of liquid near the wall, a ratio of column diameter to packing element size of at least eight should be maintained. Thus if one wishes to conduct pilot-scale packed column tests, a minimum column diameter of about 100 mm would be used together with 12-mm packing elements. The models would then permit scale-up to large columns containing 50-mm size elements of the same type, eg, Pall rings.

These models provide values of the height of a transfer unit for the liquid phase H_L and the vapor phase H_V. These values are combined to form the height of an overall transfer unit, H_{ov}:

$$H_{ov} = H_v + (m'V/L)H_L \qquad (47)$$

Table 2. **Characteristics of Packing**[a]

Packing	Nominal size, mm[b]	Surface area, m^2/m^3	Void fraction	Packing factor, F_p, m^{-1}
	Dumped (random) packing			
Intalox saddles				
ceramic				
	25	255	0.77	197
	50	118	0.79	98
metal (IMTP)	25		0.97	135
	40		0.97	79
	50		0.98	59
plastic	25	206	0.91	130
	50	108	0.93	92
	75	88	0.94	59
Berl saddles, ceramic	13	465	0.62	790
	25	250	0.68	360
	50	105	0.72	150
Pall rings				
metal	16		0.92	265
	25	205	0.94	183
	50	115	0.96	88
plastic	16	341	0.87	310
	25	207	0.90	180
	50	100	0.92	85
Raschig rings, ceramic	13	370	0.64	1902
	25	190	0.74	587
	50	92	0.74	215
	Structured packing			
Flexipac				
1	6	558	0.91	108
2	12	246	0.93	72
3	37	134	0.96	52
4	50	69	0.98	30
Sulzer-BX	6	490	>0.90	66

[a] Ref. 66.
[b] For structured packings, values correspond to crimp height.

where V and L are molar flow rates of vapor and liquid and m' is the slope of the y–x equilibrium curve (Fig. 1**b**) in the concentration range of interest. The required total height of the packed section is then obtained from the simple relationship,

$$Z_p = (N_{ov})\,(H_{ov}) \tag{48}$$

In order to determine the packed height Z_p it is necessary to obtain a value of the overall number of transfer units N_{ov}; methods for doing this are available for binary systems in any standard text covering distillation (69) and, in a more complex way, for multicomponent systems (63,78). However, it is simpler to calculate the number of required theoretical stages

and make the conversion:

$$N_{ov} = N_t(\ln m'V/L)\,(m'V/L - 1) \tag{49}$$

An alternative to determining packed height is through the use of an empirical term, height equivalent to a theoretical plate (HETP). This term can be measured in a fashion similar to that used for the overall plate efficiency of a column (eq. 44):

$$\text{HETP} = \frac{\text{total packed height}}{\text{no. of theoretical plates}} = \frac{Z_p}{N_t} \tag{50}$$

Typical experimental values of HETP for a random packing such as 50-mm Pall rings, and a structured packing, such as Intalox 2T of Norton Co., under the same system conditions, are shown in Figure 25. Many designers of packed columns prefer the use of HETP instead of H_{ov}, but the latter is more fundamental and discriminates between liquid- and vapor-phase resistances. It should be noted that terms such as H_{ov} and N_{ov} are based on vapor-phase concentrations; equivalent terms based on liquid concentrations could be used.

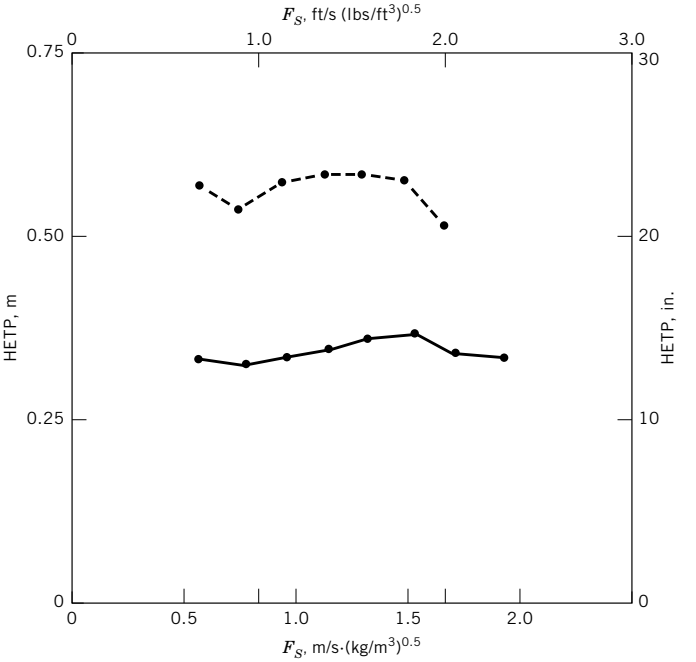

Fig. 25. Values of HETP as a function of throughput for (•– –•) 50-mm metal Pall rings and (•—•) No. 2 structured packing at 12-mm crimp height. Conditions are cyclohexane/*n*-heptane system, 165 kPa (24 psia) operating pressure, total reflux, 0.43-m diameter column. Courtesy of The University of Texas at Austin.

For structured packings, methods for predicting H_v and H_L are somewhat more reliable, partly because the fluid mechanics are less complicated than those for random packings (they can be modeled by analogy to wetted wall columns) and also because they have been extensively tested under distillation conditions and for a variety of test mixture properties. The earliest mechanistic model for structured packings appeared in 1985 (79), and has since been expanded significantly for predicting hydraulics (80) and mass transfer efficiency (81). An alternate model of Olujic (82) was developed separately, and the two models have been compared (83). For these models the key design parameters are: corrugation height, nature of metal surface, angle of corrugation from the horizontal (45 vs 60 deg) in addition to the usual physical property and flow rate considerations. Methods for predicting pressure drop and flooding in beds of structured and random packings have been reviewed (84).

4.3. Packed vs Plate Columns. Relative to plate towers, packed towers are more useful for multipurpose distillations, usually in small (under 0.5 m) towers or for the following specific applications: severe corrosion environment where some corrosion-resistant materials, such as plastics, ceramics, and certain metallics, can easily be fabricated into packing but may be difficult to fabricate into plates; vacuum operation where a low pressure drop per theoretical plate is a critical requirement; high (eg, above 49,000 kg/(h m^2) [$\sim$10,000 lb/(h ft^2)] liquid rates; foaming systems; or debottlenecking plate towers having plate spacings that are relatively close, under 0.3 m.

Plate columns have the advantage of lower fabrication cost, less dependence on good liquid and gas distribution, and protection against vapor bypassing the liquid in critical zones, eg, regions of extremely low impurities. Further, methods for the design on plate columns are somewhat more reliable than those for many of the packings, especially those packings of a proprietary nature.

There are notable cases where plate columns have been converted to packed columns to gain advantage of the low pressure drop exacted from the vapor stream. More recently the packings have been largely of the structured type. Illustrative of this is the trend toward the use of structured packing in ethylbenzene–styrene fractionators, some of which have diameters of 10 m or higher.

5. Steam Distillation

Steam distillation is used to lower the distillation temperatures of high-boiling organic compounds that are essentially immiscible with water. If an organic compound is immiscible with water, both liquids exert full vapor pressure upon vaporization from the immiscible two-component liquid. At a system pressure of P, the partial pressures would be:

$$P = p_{\text{water}} + p_{\text{organic}} \tag{51}$$

and because the water and organic compound are immiscible:

$$P = P^0{}_{\text{water}} + P^0{}_{\text{organic}} \tag{52}$$

The steam distillation of *N*-ethylaniline at atmospheric pressure (73) gives the following: the vapor pressures at 99.15°C of water and *N*-ethylaniline are 98.27 and 3.04 kPa (737 and 22.8 mm Hg), respectively. Thus, according to equation 52,

$$P = 98.27 + 3.04 = 101.3 \text{ kPa} \tag{53}$$

and the concentration of the *N*-ethylaniline in the vapor is

$$y = 3.04/101.3 = 0.030 \text{ mol fraction} \tag{54}$$

The normal boiling point of *N*-ethylaniline is 204°C. Therefore, steam distillation makes possible the distillation of *N*-ethylaniline at atmospheric pressure at a temperature of 99.15°C instead of its normal boiling point of 204°C. Commercial applications of steam distillation include the fractionation of crude tall oil (qv) (85) the distilling of turpentine (see TERPENOIDS), and certain essential oils (see OILS, ESSENTIAL).

6. Molecular Distillation

Molecular distillation occurs where the vapor path is unobstructed and the condenser is separated from the evaporator by a distance less than the mean-free path of the evaporating molecules (86). This specialized branch of distillation is carried out at extremely low pressures ranging from 13–130 mPa (0.1–1.0 μm Hg) (see VACUUM TECHNOLOGY). Molecular distillation is confined to applications where it is necessary to minimize component degradation by distilling at the lowest possible temperatures. Commercial usage includes the distillation ofvitamins (qv) and fatty acid dimers (see DIMER ACIDS).

6.1. Distillation as a Separation Method. Distillation is the most important industrial method of separation and purification of liquid components. Liquid separation methods in less common use include liquid–liquid extraction (see Extraction, Liquid–Liquid), membrane diffusion (see DIALYSIS; MEMBRANE TECHNOLOGY), ion exchange (qv), andadsorption (qv). However, distillation does not require a mass-separating agent such as a solvent, adsorbent, or membrane, and distillation utilizes energy in a convenient heating medium (often steam). Also, a wealth of experience with design and operations makes distillation column performance prediction more reliable than equivalent predictions for other methods. At times distillation also competes indirectly with methods involving solid–liquid separations such as crystallization (qv). An extensive discussion of the selection of alternative separation methods is available (29) (see SEPARATION SYSTEMS SYNTHESIS).

The suitability and economics of a distillation separation depend on such factors as favorable vapor–liquid equilibria, feed composition, number of components to be separated, product purity requirements, the absolute pressure of the distillation, heat sensitivity, corrosivity, and continuous vs batch requirements.

Distillation is somewhat energy inefficient because in the usual case heat added at the base of the column is largely rejected overhead to an ambient sink. However, the source of energy for distillations is often low-pressure steam, which characteristically is in long supply and thus relatively inexpensive. Also, schemes have been devised for lowering the energy requirements of distillation and are described in many publications (87).

6.2. Favorable Vapor–Liquid Equilibria. The suitability of distillation as a separation method is strongly dependent on favorable vapor–liquid equilibria. The absolute value of the key relative volatilities directly determines the ease and economics of a distillation. The energy requirements and the number of plates required for any given separation increase rapidly as the relative volatility becomes lower and approaches unity. For example: given an ideal binary mixture having a 50 mol% feed and a distillate and bottoms requirement of 99.8% purity each, the minimum reflux and minimum number of theoretical plates for assumed relative volatilities of 1.1, 1.5, and 4 are

Relative volatility	Minimum reflux ratio	Minimum no. of theoretical plates
1.1	20	130
1.5	4.0	31
4	0.66	9

In the example, the minimum reflux ratio and minimum number of theoretical plates decreased 14- to 33-fold, respectively, when the relative volatility increased from 1.1 to 4. Other distillation systems would have different specific reflux ratios and numbers of theoretical plates, but the trend would be the same. As the relative volatility approaches unity, distillation separations rapidly become more costly in terms of both capital and operating costs. The relative volatility can sometimes be improved through the use of an extraneous solvent that modifies the VLE. Binary azeotropic systems are impossible to separate into pure components in a single column, but the azeotrope can often be broken by an extraneous entrainer (see DISTILLATION, AZEOTROPIC AND EXTRACTIVE).

6.3. Feed Composition. Feed composition has a substantial effect on the economics of a distillation. Distillations tend to become uneconomical as the feed becomes dilute. There are two types of dilute feed cases, one in which the valuable recovered component is a low boiler and the second when it is a high boiler. When the recovered component is the low boiler, the absolute distillate rate is low but the reflux ratio and the number of plates is high. An example is the recovery of methanol from a dilute solution in water. When the valuable recovered component is a high boiler, the distillate rate, the reflux relative to the high boiler, and the number of plates all are high. An example for this case is the recovery of acetic acid from a dilute solution in water. For the general case of dilute feeds, alternative recovery methods are usually more economical than distillation.

6.4. Product Purity. Product purity requirements influence choice of separation methods. For favorable equilibria, distillation energy requirements do not increase significantly as purity specifications become tighter. For example, in an ideal binary distillation of 60 mol% of *A* in the feed, the minimum and operating reflux ratios would be essentially the same whether the required purity of *A* was 99 or 99.9999%. The number of plates would increase substantially, however, as the purity requirements became more stringent. The shortcut methods of calculating minimum reflux ratio, minimum number of plates, operating reflux ratio, and number of operating plates allow a rapid evaluation of the effect of changes in purity requirements on the key economic factors in distillation.

6.5. Operating Pressure. The absolute pressure of the distillation may have substantial economic impact. The temperature at which heat is supplied to the reboiler and removed from the condenser determines the unit cost of the energy. The cost of removing heat in the condenser increases rapidly as the condensing temperature drops below the range of air or water cooling capability; eg, the cost of removing a unit quantity of heat at −25°C may be one hundred times as high as removing it at 100°C. Similarly, the cost of the energy required for the reboiler increases rapidly as the boiler temperature increases above some level determined by local conditions. For example, at a particular site low-pressure waste steam at 110°C may be essentially without cost, but if a temperature level of 200°C is required, the unit cost of the heat is much higher. The relative cost of the heat being removed and supplied is the controlling factor determining the design of some distillations. The use of multiple interstage reboilers and condensers at different energy levels, as well as the use of other operational modes used to optimize the overall economics, has been discussed (88).

The absolute pressure may have a significant effect on the vapor–liquid equilibrium. Generally, the lower the absolute pressure, the more favorable the equilibrium. This effect has been discussed for the styrene–ethylbenzene system (29). In a given column, increasing the pressure can increase the column capacity by increasing the capacity parameter (see eqs. 42 and 43). Selection of the economic pressure can be facilitated by guidelines (89) that take into consideration the pressure effects on capacity and relative volatility. Low pressures are required for distillation involving heat-sensitive material.

6.6. Heat Sensitivity. The heat sensitivity or polymerization tendencies of the materials being distilled influence the economics of distillation. Many materials cannot be distilled at their atmospheric boiling points because of high thermal degradation, polymerization, or other unfavorable reaction effects that are functions of temperature. These systems are distilled under vacuum in order to lower operating temperatures. For such systems, the pressure drop per theoretical stage is frequently the controlling factor in contactor selection. An excellent discussion of equipment requirements and characteristics of vacuum distillation may be found in Ref. 90.

6.7. Corrosivity. Corrosivity is an important factor in the economics of distillation. Corrosion rates increase rapidly with temperature, and in distillation the separation is made at boiling temperatures. The boiling temperatures may require distillation equipment of expensive materials of construction;

however, some of these corrosion-resistant materials are difficult to fabricate. For some materials, eg, ceramics (qv), random packings may be specified, and this has been a classical application of packings for highly corrosive services. On the other hand, the extensive surface areas of metal packings may make these more susceptible to corrosion than plates. Again, cost may be the final arbiter (see CORROSION AND CORROSION CONTROL).

6.8. Batch vs Continuous Distillation. The mode of operation also influences the economics of distillation. Batch distillation is generally limited to small-scale operations where the equipment serves several different distillations.

6.9. Research. Much of the research on commercial-size distillation equipment is being done by Fractionation Research, Inc. (FRI), a nonprofit, industry-sponsored, research corporation located in Stillwater, Oklahoma. The industrial sponsors of FRI are fabricators, designers and constructors, or users of distillation equipment. The general policy of FRI has been to publish very little of the research results in the open literature. However, a number of key papers have been delivered and several of the motion pictures of operating distillation trays are available for purchase. Importantly, any proprietary reports of FRI, older than 30 years, can now be obtained from the library of Oklahoma State University at Stillwater. The released data cover literally thousands of experimental runs on large-diameter trays such as sieve, bubble-cap, and dualflow. A recent paper, co-published with FRI, provides an excellent summary of the state-of-the-art of commercial-scale distillation technology (90).

The published literature dealing with distillaiton continues at a moderate pace. Regular reviews are published by Ray (91,92) spanning the period 1967 through 1998.

7. Equipment Costs

A compilation of costs of distillation and related equipment is available (93) but must be adjusted for the effect of inflation. Some of the commercial computer-aided process design packages contain equipment cost information (see COMPUTER-AIDED DESIGN AND MANUFACTURING). For specialized internals, such as distributors, support plates, packings, crossflow plates, and so on, it is usually necessary to obtain cost information directly from the equipment vendors. It is important to recognize that the cost of a distillation system includes many components in addition to the column itself. For example, an expensive packing may be justified on the basis that it can reduce the cost of the column shell, foundations, piping, and so on. Discussions of economics of distillation systems are available (70,94).

8. Column Control

Distillation columns are controlled by hand or automatically. The parameters that must be controlled are (*1*) the overall mass balance, (*2*) the overall enthalpy balance, and (*3*) the column operating pressure. Modern control systems are

designed to control both the static and dynamic column and system variables. For an in-depth discussion, see Refs. (95–98).

9. Nomenclature

Symbol	Definition	Units
A_{12}, A_{21}	constants in the Van Laar activity coefficient equation	
B	bottoms from column	mol/s
C_{sb}	vapor capacity parameter	m/s
D	distillate from column	mol/s
E_o	overall column plate efficiency (eq. 44)	fractional
E_{mv}	Murphree plate efficiency (eq. 45)	fractional
E_{og}	local, or point, efficiency based on vapor concentrations	fractional
f	fugacity	kPa
F	feed	mol/s
F^*	F-factor (eq. 43)	$\mathrm{m/s \cdot (kg/m^3)^{0.5}}$
$F_A{}^*$	F-factor based on active (bubbling) area	$\mathrm{m/s \cdot (kg/m^3)^{0.5}}$
$F_H{}^*$	F-factor based on hole area	$\mathrm{m/s \cdot (kg/m^3)^{0.5}}$
F_p	packing factor from Table 2	1/m
G	gas mass rate	kg/s
$\overline{H}$;	enthalpy per mole	
H	enthalpy per unit time	
H^*	Henry's law constant (eq. 17)	kPa/mol fraction
HETP	height equivalent of theoretical plate	m
H_L	height of a liquid-phase transfer unit	m
H_{ov}	height of an overall transfer unit, vapor concentrations	m
H_v	height of a vapor-phase transfer unit	m
K	y^*/x, vapor–liquid equilibrium ratio (eq. 1)	
L	liquid rate	mol/s
$\underline{L}$	average liquid rate for section	mol/s
$\overline{L}$;	liquid mass rate	kg/s
m	an equilibrium stage below the feed	
m'	slope of equilibrium line	
n	an equilibrium stage above the feed	
N	number of stages	
N^*	number of components	
N_a	number of actual stages	
N_{ov}	number of transfer units, vapor concentration basis	
N_t	number of theoretical stages	
P	total pressure of system	kPa
p	partial pressure	kPa
P^0	vapor pressure	kPa
q	heat to vaporize 1 mol feed divided by molal latent heat of feed (eq. 36)	
$\overline{q}$;	heat removed or added at column auxiliaries	
R	reflux	mol/s
R'	gas law constant	
T	temperature	K
v	vapor molar volume	$\mathrm{m^3/mol}$
V	vapor molar rate	mol/s
$\overline{V}$;	average molar vapor rate for section	mol/s
V^*	vapor velocity	m/s
x	mole fraction in liquid	
y	mole fraction in vapor	
y^*	mole fraction vapor in equilibrium with x	

Symbol	Definition	Units
z	compressibility factor in gas law	
Z_p	height of packed bed	m
α	relative volatility (eq. 2)	
γ^{L}	liquid-phase activity coefficient (eq. 6)	
γ^{∞}	terminal activity coefficient, at infinite dilution	
$\Lambda_{12}, \Lambda_{21}$	constant in Wilson activity coefficient model (eq. 13)	
ρ	fluid-phase density	kg/m^3
ϕ	fugacity coefficient (eq. 20)	
	Superscripts	
B	bottoms	
C	condenser	
D	distillate	
E	end	
F	feed	
f	feed stage	
L	liquid	
m	stage number m	
$m-1$	stage below m	
$m+1$	stage above m	
n	stage number n	
$n-1$	stage below n	
$n+1$	stage above n	
N	Nth component of components i to n	
P	pressure	
S	reboiler	
T	top column	
V	vapor	
	Subscripts	
1,2,3 . . . n	component numbers	
B	bottoms	
D	distillate	
F	feed	
g	gas	
H	component H of binary system L–H, H is the high boiler	
i,j	components of mixture 1 . . . i,j, . . . n	
L	component L of binary system L–H, L is the low boiler	
L	liquid	
min	minimum	
P	pressure	
R	rectifying section	
S	stripping section	
T	temperature	

BIBLIOGRAPHY

"Distillation" in *ECT* 1st ed., Vol. 5, pp. 156–187, by E. G. Scheibel, Hoffmann-LaRoche, Inc.; in *ECT* 2nd ed., Vol. 7, pp. 204–248, by C. D. Holland and J. D. Lindsey, Texas A & M University; in *ECT* 3rd ed., Vol. 7, pp. 849–891, by E. R. Hafslund, E. I. du Pont de Nemours & Co., Inc.; in *ECT* 4th ed., Vol. 8, pp. 311–358, by James R. Fair,

The University of Texas at Austin; "Distillation" in *ECT* (online), posting date: December 4, 2000, by James R. Fair, The University of Texas at Austin.

CITED PUBLICATIONS

1. A. J. V. Underwood, *Trans. I. Chem. E.* **13**, 34 (1935).
2. J. R. Fair, *AIChE Symp. Ser. No. 235* **79**, 1 (1984).
3. J. Gmehling, U. Onken, and W. Arlt, *Vapor–Liquid Equilibrium Collection* (continuing series), DECHEMA, Frankfurt, Germany, 1979.
4. M. Hirata, S. Ohe, and K. Nagahama, *Computer Aided Data Book of Vapor–Liquid Equilibria*, Elsevier, Amsterdam, The Netherlands, 1975.
5. E. Hala, J. Pick, V. Fried, and O. Vilim, *Vapor–Liquid Equilibrium*, 2nd ed., Pergamon Press, Oxford, UK, 1967.
6. E. Hala, I. Wichterle, J. Polak, and T. Boublik, *Vapor–Liquid Equilibrium at Normal Pressures*, Pergamon Press, Oxford, UK, 1968.
7. I. Wichterle, J. Linek, and E. Hala, *Vapor–Liquid Equilibrium Data Bibliography*, Elsevier, Amsterdam, The Netherlands, 1975.
8. A. Fredenslund, J. Gmehling, and P. Rasmussen, *Vapor–Liquid Equilibria Using UNIFAC*, Elsevier, Amsterdam, The Netherlands, 1977.
9. J. H. Hildebrand, J. M. Prausnitz, and R. L. Scott, *Regular and Related Solutions*, Van Nostrand Reinhold Co., Inc., New York, 1970.
10. E. L. Derr and C. H. Deal, *I. Chem. E. Symp. Ser. No. 32* **3**(40), (1969).
11. D. A. Palmer, *Handbook of Applied Thermodynamics*, CRC Press, Inc., Boca Raton, Fla., 1987.
12. J. M. Prausnitz, R. N. Lichtenthaler, and E. G. Azeredo, *Molecular Thermodynamics of Fluid-Phase Equilibria*, 3rd ed., Prentice-Hall, Inc., Englewood Cliffs, N.J., 1999.
13. R. C. Reid, J. M. Prausnitz, and B. Pohling, *The Properties of Gases and Liquids*, 4th ed., McGraw-Hill Book Co., Inc., New York, 1987.
14. S. M. Walas, *Phase Equilibria in Chemical Engineering*, Butterworths, Reading, Mass., 1998.
15. J. D. Seader, *Separation Process Principles*, John Wiley & Sons, Inc., New York, 1981.
16. P. Wankat, *Equilibrium-Staged Separations*, Elsevier Science Publishing Co., Inc., New York, 1988.
17. M. Van Winkle, *Distillation*, McGraw-Hill Book Co., Inc., New York, 1967.
18. J. J. Van Laar, *Z. Physik. Chem.* **72**, 723 (1910); **83**, 599 (1913).
19. G. M. Wilson, *J. Am. Chem. Soc.* **86**, 127 (1964).
20. H. Renon and J. M. Prausnitz, *AIChE J.* **14**, 135 (1968).
21. D. S. Abrams and J. M. Prausnitz, *AIChE J.* **21**, 116 (1975).
22. Margules, *Sitzber. Math.-Naturw. Kl. Kaiserlichen Akad. Wiss. (Vienna)* **104**, 1243 (1895).
23. H. H. Chien and H. R. Null, *AIChE J.* **18**, 1177 (1972).
24. J. M. Prausnitz and co-workers, *Computer Calculations for Multicomponent Vapor–Liquid and Liquid–Liquid Equilibria*, Prentice-Hall, Inc., Englewood Cliffs, N.J., 1980.
25. *Technical Data Book, Petroleum Refining*, 3rd ed., Vols. **I** and **II**, American Petroleum Institute, New York, 1976.
26. Y.-L. Huang, J. D. Olson, and G. E. Keller, *Ind. Eng. Chem. Research* **31**, 1759 (1992).
27. J. Gmehling et al. *Azeotropic Data*, Wiley/VCH, New York, 1994. (**2** Vols.)
28. L. Horsley, *Azeotropic Data—III*, Advances in Chemistry Series No. 116, American Chemical Society, Washington, D.C., 1973.

29. C. J. King, *Separation Processes*, 2nd ed., McGraw-Hill Book Co., Inc., New York, 1980.
30. W. L. McCabe and E. W. Thiele, *Ind. Eng. Chem.* **17**, 605 (1925).
31. M. Ponchon, *Tech. Mod.* **13**, 20, 55 (1921).
32. R. Savarit, *Arts Metiers* **65**, 145, 178, 266, 307 (1922).
33. M. R. Fenske, *Ind. Eng. Chem.* **24**, 482 (1932).
34. A. J. V. Underwood, *Chem. Eng. Progr.* **44**, 603 (1948).
35. J. R. Fair and W. L. Bolles, *Chem. Eng.* **75**(9), 156 (Apr. 22, 1968).
36. G. G. Brown and co-workers, *Unit Operations*, John Wiley & Sons, Inc., New York, 1950.
37. E. R. Gilliland, *Ind. Eng. Chem.* **32**, 918 (1940).
38. J. H. Erbar and R. N. Maddox, *Petrol. Ref.* **40**(5), 183 (1961).
39. H. E. Eduljee, *Hydrocarbon Proc.* **54**(9), 120 (1975).
40. E. W. Thiele and R. L. Geddes, *Ind. Eng. Chem.* **25**, 290 (1933).
41. C. D. Holland, *Fundamentals of Multicomponent Distillation*, McGraw-Hill Book Co., Inc., New York, 1981.
42. R. N. S. Rathore, K. A. Van Wormer, and G. J. Powers, *AIChE J.* **20**, 491 (1974).
43. D. C. Freshwater and B. D. Henry, *Chem. Eng. (London)* (**301**), 533 (1975).
44. J. E. Hendry, D. F. Rudd, and J. D. Seader, *AIChE J.* **19**, 1 (1973).
45. W. L. Bolles, in B. D. Smith, ed., *Design of Equilibrium Stage Processes*, McGraw-Hill Book Co., Inc., New York, 1963, Chapt. 14.
46. M. H. Hutchinson and R. F. Baddour, *Chem. Eng. Progr.* **52**(12), 503 (1956).
47. F. Kastanek, M. V. Huml, and V. Braun, *I. Chem. E. Symp. Ser. No. 32*, **5**(100), (1969).
48. W. V. Delnicki and J. L. Wagner, *Chem. Eng. Progr.* **52**(1), 28 (1956).
49. J. R. Fair, Chapt. 5 in *Handbook of Separation Process Technology*, R. W. Rousseau, ed., John Wiley, New York, 1987.
50. J. R. Fair, in R. H. Perry and D. Green, eds., *Perry*'s Chemical Engineers' Handbook, 7th ed., McGraw-Hill Book Co., Inc., New York, 1997, section 14.
51. *Bubble-Tray Design Manual*, American Institute of Chemical Engineers (AIChE), New York, 1958.
52. H. Chan and J. R. Fair, *Ind. Eng. Chem. Proc. Des. Devel.* **23**, 814, 820 (1984).
53. M. J. Lockett, *Distillation Tray Fundamentals*, Cambridge University Press, Cambridge, Mass., 1986.
54. M. M. Dribika and M. W. Biddulph, *Trans. I. Chem. E.* **70**, Part A, 142 (1992).
55. M. Prado and J. R. Fair, *Ind. Eng. Chem. Res.* **29**, 1031 (1990).
56. K. E. Porter, M. J. Lockett and C. T. Lim*Trans. I. Chem. E.* **50**, 91 (1972).
57. W. V. Pincezewski, N. D. Benke, and C. J. D. Fell, *AIChE J.* **21**, 1210 (1975).
58. K. E. Porter, A. Safekouri, and M. J. Lockett, *Trans. I. Chem. E.* **51**, 265 (1973).
59. M. Prado, K. L. Johnson, and J. R. Fair, *Chem. Eng. Progr.* **83**(3), 32 (1987).
60. J. A. Garcia and J. R. Fair, *Ind. Eng. Chem. Res.* **39**, 1809, 1818 (2000).
61. H. E. O'Connell, *Trans. AIChE* **42**, 741 (1946).
62. R. Krishna, H. F. MartinezR. Sreedhar, and G. L. Standart, *Trans. I. Chem. E.* **55**, 178 (1977).
63. R. Taylor and R. Krishna *Multicomponent Mass Transfer*, John Wiley, New York, 1993.
64. A. Sperandio, M. Richard, and M. Huber, *Chem.-Ing.-Tech.* **37**, 22 (1965).
65. W. D. Stoecker and B. Weinstein, *Chem. Eng. Progr.* **73**(11), 71 (1977).
66. R. F. Strigle, *Packed Tower Design and Applications*, Gulf Publishing, Houston, Tex., 1994.
67. J. R. Fair and J. L. Bravo, *Chem. Eng. Progr.* **86**(1), 19 (1990).
68. P. J. Hoek, J. A. Wesselingh, and F. J. Zuiderweg, *Chem. Eng. Res. Des.* **64**, 431 (1986).

69. R. E. Treybal, *Mass Transfer Operations*, 3rd ed., McGraw-Hill., Inc., New York, 1980.
70. H. Z. Kister, *Distilation—Design*, McGraw-Hill, Inc., New York, 1992.
71. J. Stichlmair and J. R. Fair *Distilation—Principles and Practices*, Wiley-VCH, New York, 1998.
72. P. A. Schweitzer, ed., *Handbook of Separation Techniques for Chemical Engineers*, 3rd ed., McGraw-Hill Book Co., Inc., New York, 1997,
73. R. W. Rousseau, ed., *Handbook of Separation Process Technology*, John Wiley & Sons, Inc., New York, 1987, Chapt. 5.
74. T. K. Sherwood, G. H. Shipley, and F. A. L. Holloway, *Ind. Eng. Chem.* **30**, 765 (1938).
75. M. Leva, *Chem. Eng. Progr. Symp. Ser. No. 10* **50**, 51 (1954).
76. W. L. Bolles and J. R. Fair, *Chem. Eng.* **89**(14), 109 (July 12, 1982).
77. J. L. Bravo and J. R. Fair, *Ind. Eng. Chem. Proc. Des. Dev.* **21**, 162 (1982).
78. R. Krishnamurthy and R. Taylor, *AIChE J.* **31**, 449, 456 (1985).
79. J. L. Bravo, J. A. Rocha, and J. R. Fair, *Hydrocarbon Proc.* **64**(1), 91 (1985).
80. J. A. Rocha, J. L. Bravo, and J. R. Fair, *Ind. Eng. Chem. Res.* **32**, 641 (1993).
81. J. A. Rocha, J. L. Bravo, and J. R. Fair, *Ind. Eng. Chem. Res.* **35**, 1660 (1996).
82. Z. Olujic, *Chem. Biochem. Eng.* **11**, 31 (1997).
83. J. R. Fair, A. F. Seibert, M. Behrens, P. P. Saraber, and Z. Olujic, *Ind. Eng. Chem. Res.* **39**, 1788 (2000).
84. J. Stichlmair, J. L. Bravo and J. R. Fair, *Gas Sepn. Purif.* **3**, 19 (1989).
85. J. Drew and M. Propst, eds., *Tall Oil*, Pulp Chemicals Association, New York, 1981.
86. K. C. D. Hickman, in R. H. Perry and C. H. Chilton, eds., *Chemical Engineers'* Handbook, 5th ed., McGraw-Hill Book Co., Inc., New York, 1973, section 13.
87. J. R. Fair, in Y. A. Liu, H. A. McGee, and W. R. Epperly, eds., *Recent Developments in Chemical Process and Plant Design*, John Wiley & Sons, Inc., New York, 1987, Chapt. 3.
88. W. C. Petterson and T. A. Wells, *Chem. Eng.* **84**(20), 79 (1977).
89. H. Z. Kister and I. D. Doig, *Hydrocarbon Proc.* **56**(7), 132 (1977).
90. J. G. Kunesh, H. Z. Kister, M. J. Lockett and J. R. Fair, *Chem. Eng. Prog.* **91**(10), 43 (1995).
91. M. S. Ray, *Chemical Engineering Bibliography, 1967–1988*, Noyes Publications, Park Ridge, N.J., 1990.
92. M. S. Ray, *Sepn. Sci. Technol.* **34**, 3305 (1999). Also, *Sepn. Sci. Technol.* **34**, 139 (1999); **32**, 3067 (1997); **32**, 1163 (1997).
93. M. Peters and K. D. Timmerhaus, *Plant Design and Economics for Chemical Engineers*, 4th ed., McGraw-Hill Book Co., Inc., New York, 1991.
94. H. Z. Kister, *Distillation–Operation*, McGraw-Hill., Inc., New York, 1990.
95. A. E. Nisenfeld and R. C. Seeman, *Distillation Columns*, Instrument Society of America, Research Triangle Park, N.C., 1981.
96. F. G. Shinskey, *Distillation Control*, 2nd ed., McGraw-Hill Book Co., Inc., New York, 1984.
97. P. B. Deshpande, *Distillation Dynamics and Control*, Instrument Society of America, Research Triangle Park, N.C., 1984.
98. P. S. Buckley, W. L. Luyben, and J. P. Shunta, *Design of Distillation Control Systems*, Instrument Society of America, Research Triangle Park, N.C., 1985.

JAMES R. FAIR
The University of Texas at Austin